

O. Kempf · A. Matter · D. W. Burbank · M. Mange

Depositional and structural evolution of a foreland basin margin in a magnetostratigraphic framework: the eastern Swiss Molasse Basin

Received: 11 March 1998 / Accepted: 12 March 1999

Abstract This integrated study of the sedimentology, magnetostratigraphic chronology and petrography of the mostly continental clastics of the Oligocene to Miocene Swiss Molasse Basin underpins a reconstruction of facies architecture and delineates relationships between the depositional evolution of a foreland-basin margin and exhumation phases and orogenic events in the adjacent orogen. A biostratigraphically based high-resolution magnetostratigraphy provides a detailed temporal framework and covers nearly the whole stratigraphic record of the Molasse Basin (31.5–13 Ma). Three transverse alluvial fan systems evolved at the southern basin margin. They are characterized by distinct petrographic compositions and document the exhumation and denudation history of the growing eastern Swiss Alps. Enhanced northward propagation of the orogenic wedge is interpreted to have occurred between 31.5 and 26 Ma. During the period 24–19 Ma, intense in-sequence and out-of-sequence thrusting took place as Molasse strata were accreted to the orogenic wedge. A third active tectonic phase, possibly caused by backthrusting of the Plateau Molasse, probably occurred between ca. 15 and 13 Ma. Fan head migration between 31.5 and 13 Ma is probably controlled by the structural evolution of the thrust front due to Molasse accretion and backthrusting.

Key words Molasse Basin · Alpine tectonics · Alluvial sedimentation · Magnetostratigraphy · Foreland basin evolution

Introduction

The Molasse Basin is a classical foredeep at the northern side of the Alps. Displaying a highly asymmetrical cross section with a thick clastic succession, it exceeds 4 km in the south and feathers out towards the north (Fig. 1). It is widely accepted that the structural development of the orogenic wedge controls the geometry and shape of the foreland basin and therefore has strong influence on the facies distribution within the basin (Beaumont 1981; Jordan 1981); hence, the stratigraphy of a foreland basin reflects the tectonic evolution of the adjacent orogen.

The stratigraphy and the facies relationships of the Molasse have been studied intensely over the past decades (e.g., Homewood and Allen 1981; Allen et al. 1985; Berger 1985; Diem 1986; Keller 1989; Schoepfer 1989; Schlunegger et al. 1993), but the causal linkages between the tectonic evolution of the Alps and the stratigraphic record in the basin (Homewood et al. 1986; Pfiffner 1986; Sinclair et al. 1991; Sinclair and Allen 1992) have remained obscure due to uncertainties in the chronological record. Now a newly established high-resolution magnetostratigraphy in the Swiss Molasse Basin provides a very detailed chronostratigraphic framework (Burbank et al. 1992; Schlunegger et al. 1996; Kempf et al. 1997). Based on this, Schlunegger et al. (1997b) have established a close temporal link of the relationships between the Alpine orogeny and the Molasse Basin evolution on a transect across the central Swiss Molasse Basin.

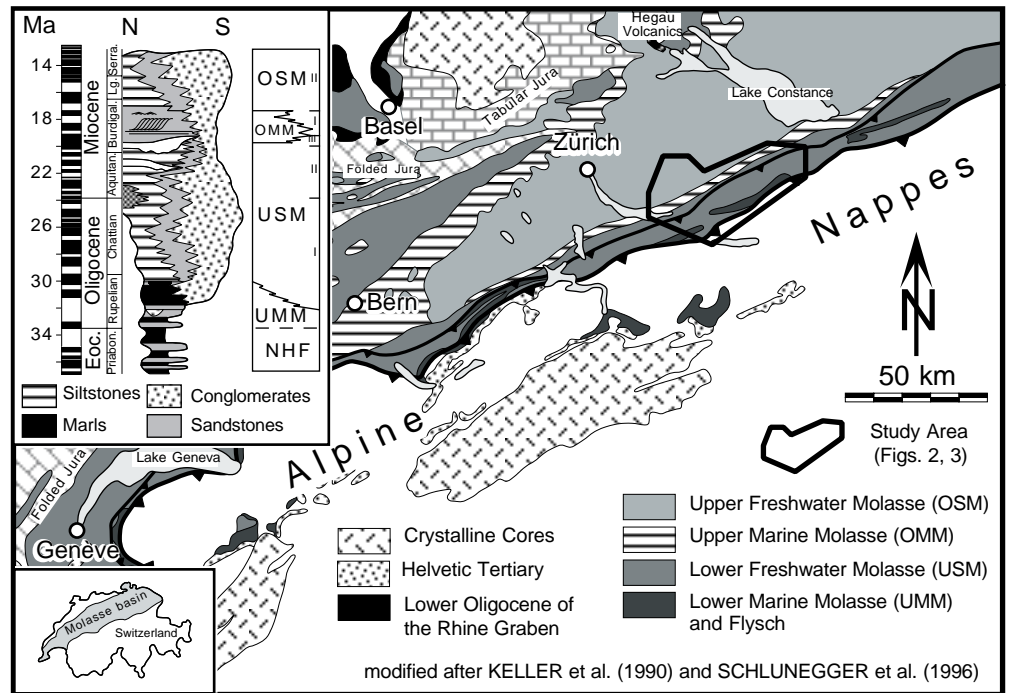
The aim of this study is to reconstruct the depositional and structural evolution of the Molasse of eastern Switzerland. In particular, we use high-resolution magnetostratigraphy to tie the sedimentary, structural, and geometrical evolution of the proximal

O. Kempf (✉) · A. Matter
Geologisches Institut, Universität Bern, Baltzerstrasse 1,
CH-3012 Bern, Switzerland
e-mail: oliver.kempf@geo.unibe.ch,
Tel.: +41-31-6318759,
Fax: +41-31-6314843

D. W. Burbank
Department of Geosciences, Pennsylvania State University,
University Park, PA 16802, USA

M. Mange
Department of Earth Sciences, University of Oxford,
Parks Road, Oxford, OX1 3PR, England

Fig. 1 Geological bedrock map of the Swiss Molasse Basin and schematic stratigraphy and age of the eastern Molasse and North Helvetic Flysch (NHF) in a north-south cross section. USM I-III and OSM I-II refer to informal sub-units (see text). The study area is outlined



Molasse. Different dispersal systems and their catchment areas were identified using heavy mineral suites of sandstones and the clast composition of conglomerates. The geometry and the location of these dispersal systems in the basin were mapped to reconstruct shifts of depositional systems. The combined information about the stratal architecture in the basin and the structural evolution in the source terrain allows an improved understanding about the relationships between thrusting and exhumation in the Alps and the sedimentary processes in the Molasse Basin.

Geological setting

Five lithostratigraphic units classically subdivide the North Alpine Foreland Basin (Matter et al. 1980; Keller 1989; Sinclair et al. 1991) for which we use the German abbreviations; these are the North Helvetic Flysch (NHF), the Lower Marine Molasse (UMM), the Lower Freshwater Molasse (USM), the Upper Marine Molasse (OMM), and the Upper Freshwater Molasse (OSM; Fig. 1). The Molasse deposits form two shallowing-, coarsening-, and thickening-upward megasequences. The first megasequence consists of the deep marine NHF (Priabonian), the marine UMM (Rupelian) and the USM (Rupelian to lower Burdigalian), a thick succession of fluvial clastics (Fig. 1). The Burdigalian age of the youngest USM deposits in the study area (Kempf et al. 1997) contrasts with the western part of the Swiss Molasse Basin, where the youngest deposits of the USM comprise Aquitanian strata (20 Ma; Berger 1985; Schlunegger et al. 1996). The second megasequence starts with the Burdigalian trans-

gression and consists of shallow-marine sand- and siltstones of the OMM interfingering with large fan deltas at the southern basin margin (Keller 1989; Schaad et al. 1992; Bolliger et al. 1995), followed by fluvial clastics of the OSM (Burdigalian to Serravallian). These lithostratigraphic units, however, are strongly heterochronous both from west to east and from south to north (Diem 1986; Keller 1989; Schlunegger et al. 1996).

Following Schlanke (1974) and Kempf et al. (1997), the Molasse units of eastern Switzerland are informally subdivided into subunits that are based on the heavy mineral content of the sandstones and, if obtainable, the clast composition of the conglomerates: USM I (Rupelian-Chattian), USM II (Aquitainian), USM III (lower Burdigalian), OSM I (Burdigalian, continental equivalent to the marine OMM), and OSM II (Langhian-Serravallian; Fig. 1). The subunit USM III is only of local significance (eastern Swiss Molasse; Kempf et al. 1997) and corresponds temporally to the lowermost OMM of central Switzerland (basal Luzern Formation of Keller 1989).

The study area is located in eastern Switzerland between Lake Zurich and the Rhine valley and covers the proximal part of the Molasse Basin, including the Subalpine Molasse as well as the southern part of the Plateau Molasse (Figs. 1, 2). Here, the Molasse deposits are well exposed and provide excellent insight into the tectonic structure of the southern basin margin (Fig. 3). Two major thrust sheets make up the northern and eastern part of the Subalpine Molasse (Kronberg and Gäbris thrust sheets, Fig. 2C). The southern area is more disrupted and consists of two larger thrust sheets (Schorhüttenberg and Speer thrust sheets; Fig. 2C) and three smaller, internally disturbed thrust sheets

(Habicht 1945a). The northward dip of the upwarped strata of the Plateau Molasse is interpreted to be caused by a south-vergent backthrust as a consequence of imbrication of the southward-dipping thrust sheets of the Subalpine Molasse (triangle zone; Stäuble and Pfiffner 1991).

Methods

Depositional systems

Based on detailed sedimentological logging in the Subalpine Molasse (USM; Kempf 1998) and the OSM lithofacies classification of Bürgisser (1981), five depositional systems define the megascopic architecture of the alluvial Molasse deposits (USM, OSM) according to Schlunegger et al. (1997c; Fig. 2B).

Floodplain depositional systems commonly consist of laminated to massive mudstones, often showing pedogenic features of high maturity (root traces, red-violet mottling), abundant caliche nodules, and fine- to medium-grained sandstones, that are interpreted as crevasse splays or channels. Massive sandstone channels are of minor importance.

Sandstone channel-belt depositional systems comprise single or stacked medium-to-coarse channelized sandstone bodies of 2 to >15 m thickness (sandstone/siltstone facies association [H3] of Bürgisser 1981). They show an erosive base with pebble lags and rip-up clasts. These alternate with floodplain deposits that show less mature pedogenic features.

Conglomerate channel-belt depositional system in a more proximal position consists of >2-m-thick conglomerate beds interbedded with mature floodplain fines (conglomerate/siltstone facies association [H2] of Bürgisser 1981). The conglomerates form amalgamated units up to 20 m thick that can be traced laterally for several hundred meters. The clast size of the conglomerates is usually less than 20 cm. Alluvial megafan depositional systems (conglomerate facies association [H1] of Bürgisser 1981) consist almost entirely of massive, crudely horizontally bedded conglomerates with a clast size up to 60 cm. Finer-grained sediments are only rarely preserved as thin, laterally restricted units. Occasionally mass flows are present in the most proximal facies.

Bajada depositional systems occur locally on the flanks and on top of the alluvial megafan conglomerates. They consist of thick, fine-grained massive debris flows and narrow, ribbon-like channels with a chaotic conglomerate fill and deep scours. The conglomerates exhibit outsized clasts of more than 70 cm. They were presumably deposited by hyperconcentrated flows. Sandstone bodies are subordinate. The conglomerates are also amalgamated to larger channelized bodies and may even form a small 3- to 4-km-wide independent fan. The bajada deposits occur only locally and their petrographic composition indicates that they are

derived directly from the thrust front (Habicht 1945a).

We add a marine depositional system that comprises all marine deposits of UMM and OMM (Fig. 2B). These deposits include offshore marls and coastal sandstones of the UMM (Frei 1979; Diem 1986) as well as shallow-marine silt- and sandstones of the OMM (Keller 1989).

Sedimentary petrography

For the identification of different dispersal systems, sandstones were sampled along the magnetostratigraphic sections and analyzed for the heavy mineral composition according to Füchtbauer (1958, 1964) and Matter (1964). Data published by Hofmann (1957) and Füchtbauer (1964) were included to complete the petrographic record. We quantitatively studied the clast composition of the conglomerates in order to distinguish between different alluvial fans and to recognize their catchment areas, including data from Renz (1937a) and Habicht (1945a). For the quantitative clast analysis the reader is referred to Schlunegger et al. (1993).

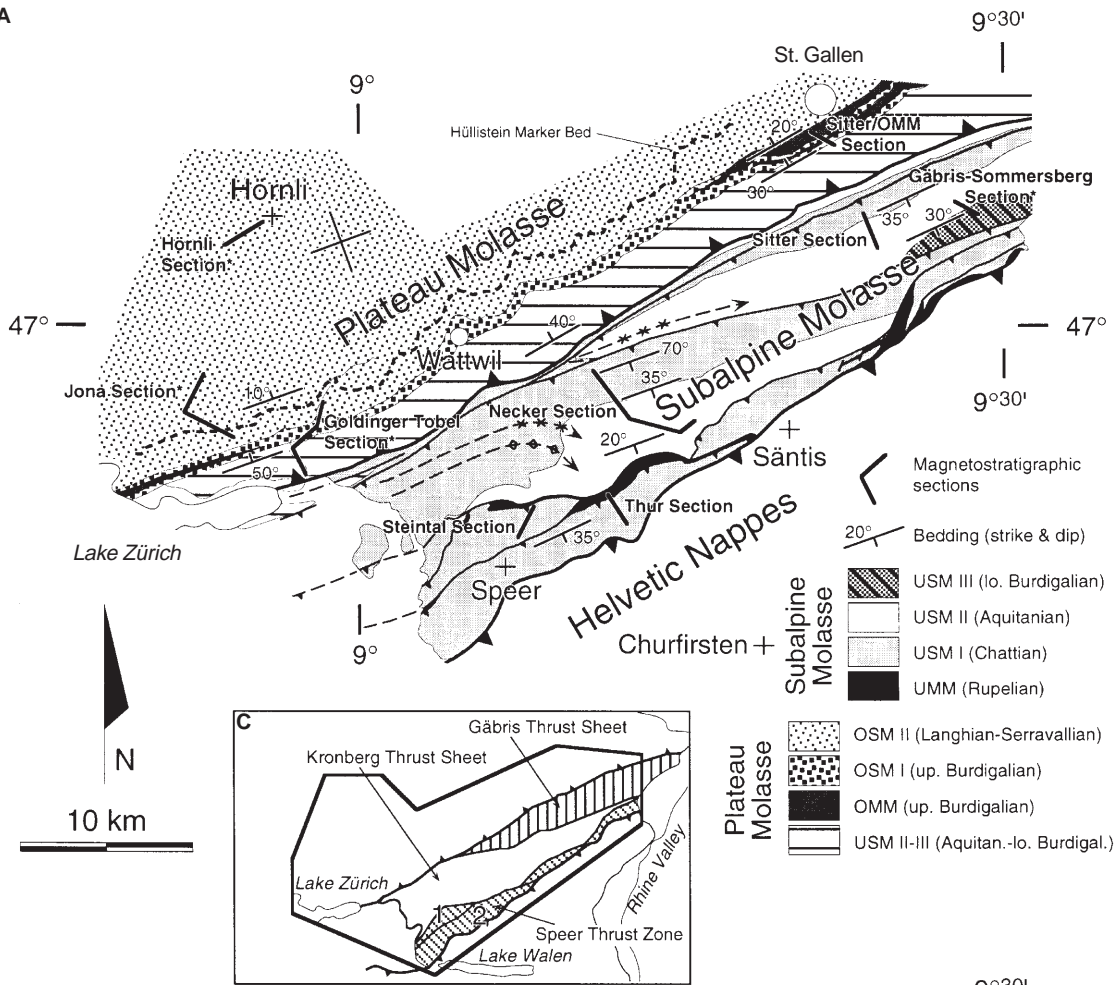
Palinspastic restoration

To understand the paleogeographic evolution of the southern basin margin, the allochthonous units of the Molasse had to be restored palinspastically to their position during deposition. The restoration of the Subalpine Molasse of eastern Switzerland is largely based on the stratigraphic and structural interpretation of a seismic line (Stäuble and Pfiffner 1991; Pfiffner et al. 1997a) in combination with outcrop data. These data suggest a shortening of ca. 28 km, the presence of a stack of imbricate thrust sheets that flatten towards the south, and a probable N-S extension of USM deposits beneath the Alpine nappes (Fig. 3A). Moreover, the presence of a triangle zone is evident from seismic data (Stäuble and Pfiffner 1991). Other interpreted seismic lines constrained by borehole data (Central Switzerland: Vollmayr and Wendt 1987; Southern Germany and Austria: Müller et al. 1988; Schwerd et al. 1995; Vollmayr and Jäger 1995) show a similar tectonic structure of the Subalpine Molasse. Tectonic interpretations based on balanced cross sections lead to a similar amount of shortening of the Subalpine Molasse (Burkhard 1990; Pfiffner et al. 1997a). Due to lateral changes of the tectonic structure, the palinspastic restoration in the western part of the study area may not apply to the entire study area (Fig. 3C).

Magnetostratigraphy

Nine sections were sampled for magnetostratigraphy in the Subalpine Molasse and Plateau Molasse of eastern

A



B

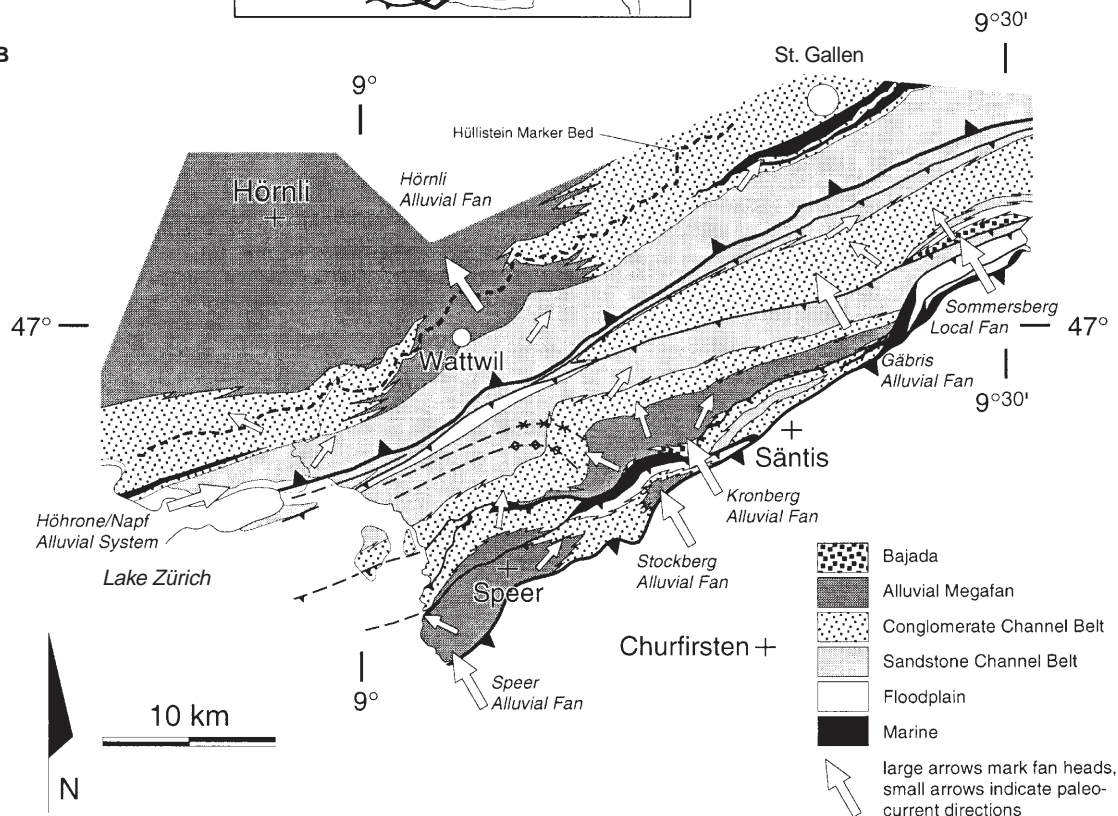


Fig. 2 A Tectono-stratigraphic map of the study area (modified after Kempf et al. 1997) and locations of the magnetostratigraphic sections. *Marked sections* are discussed in Kempf et al. (1997). **B** Facies map showing the distribution of the depositional systems in the study area. Palaeocurrent directions (*small arrows*) indicate radial (fan-shaped geometry) and basin-axial drainage systems. **C** Tectonic map of the eastern Swiss Subalpine Molasse. The Schorhüttenberg Thrust Sheet (1) and the Speer Thrust Sheet (2) are part of the Speer Thrust Zone. The maps are based mainly on data from Saxer (1938), Renz (1937a, 1937b), Habicht (1945a, 1945b), Ludwig et al. (1949), Büchi (1950), Ochsner (1975) and Bürgisser (1981)

Switzerland (Fig. 2A) comprising 586 sites and a total measured thickness of ca. 12.5 km. Four to six oriented samples, predominantly mudstones and rarely fine-grained sandstones, were collected from each site. The demagnetization behavior for representative samples of each analyzed section was identified in a pilot study by thermal and alternating field demagnetization. The samples were taken from various stratigraphic levels and depositional systems (see Schlunegger et al. 1996 for justification) and analyzed using a cryogenic magnetometer. Thermal demagnetization was carried out in steps of 50 °C from room temperature to 550 °C, and in steps of 30 °C from 550° to 640 °C. After each temperature step, the magnetic susceptibility was measured to

identify growth of magnetic minerals during sample processing. We identified a stable direction of the demagnetization vector between 200 and 350 °C that is interpreted as the characteristic remanent magnetization (Butler 1992). Therefore, we demagnetized and measured the remaining samples at three heating steps between 200° and 350 °C. Fisher statistics (Fisher 1953) were used to test the coherency of the magnetic directions for each site. Groups of three samples were classified “class I” if $k \geq 10$ and “class II” if $k < 10$, or two samples yielded an unambiguous polarity with $k \geq 10$. The mean magnetic vector of each site was used to calculate the virtual geomagnetic pole (VGP; Fisher 1953) including an α_{95} error envelope for each VGP latitude. Kempf et al. (1997) give a detailed description on the paleomagnetic processing and discuss the magnetostratigraphy of the Hörnli, Jona, Goldinger Tobel, and Gäbris-Sommersberg sections. The localities of the individual magnetostratigraphic sections are shown on Fig. 2A. For more detailed information about the paleomagnetic data and location of the sites the reader is referred to Kempf (1998).

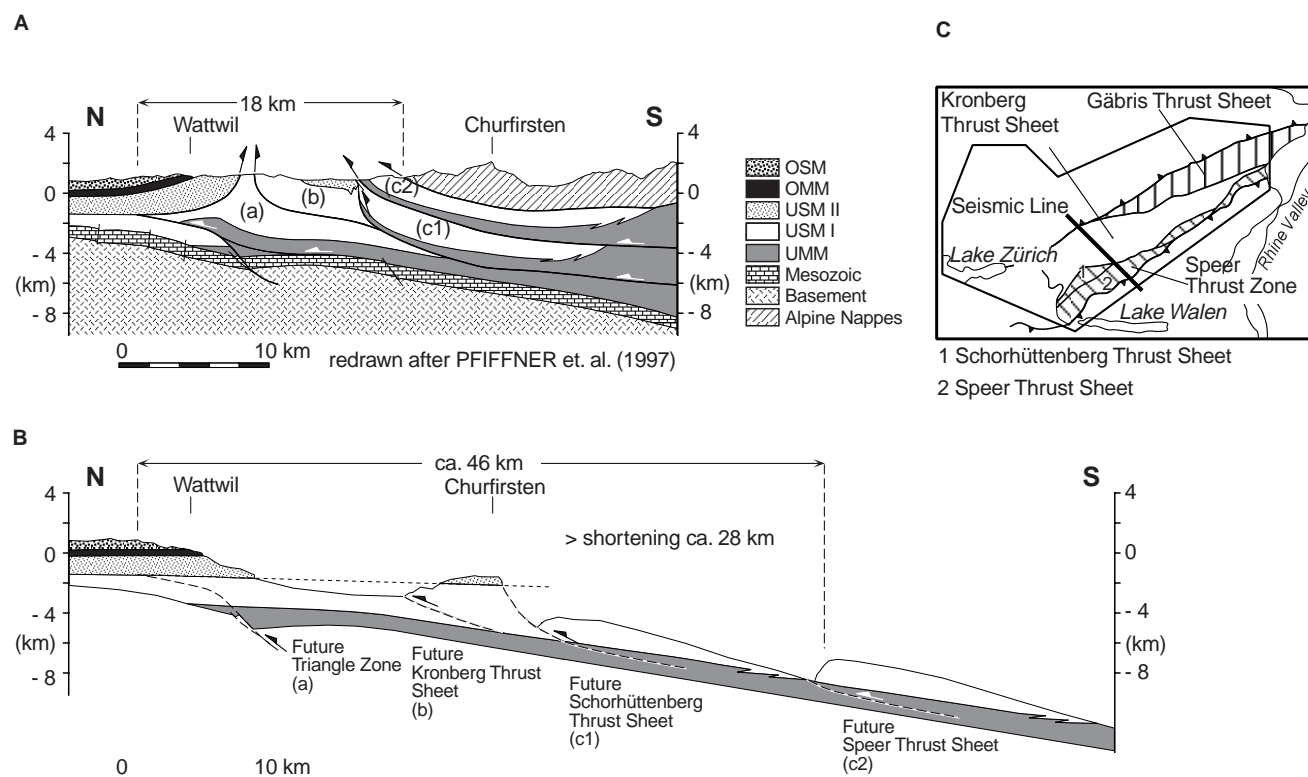
Results

Magnetostratigraphic framework

Magnetostratigraphic calibration of micro-mammal faunas

Well-correlated magnetostratigraphic sections that contain micro-mammal-bearing sites have been used to

Fig. 3 A Cross section through the eastern Swiss Subalpine Molasse. **B** Palinspastic restoration. The amount of shortening within the Subalpine Molasse is ca. 28 km. **C** Location of the seismic line of Pfiffner et al. (1997a)



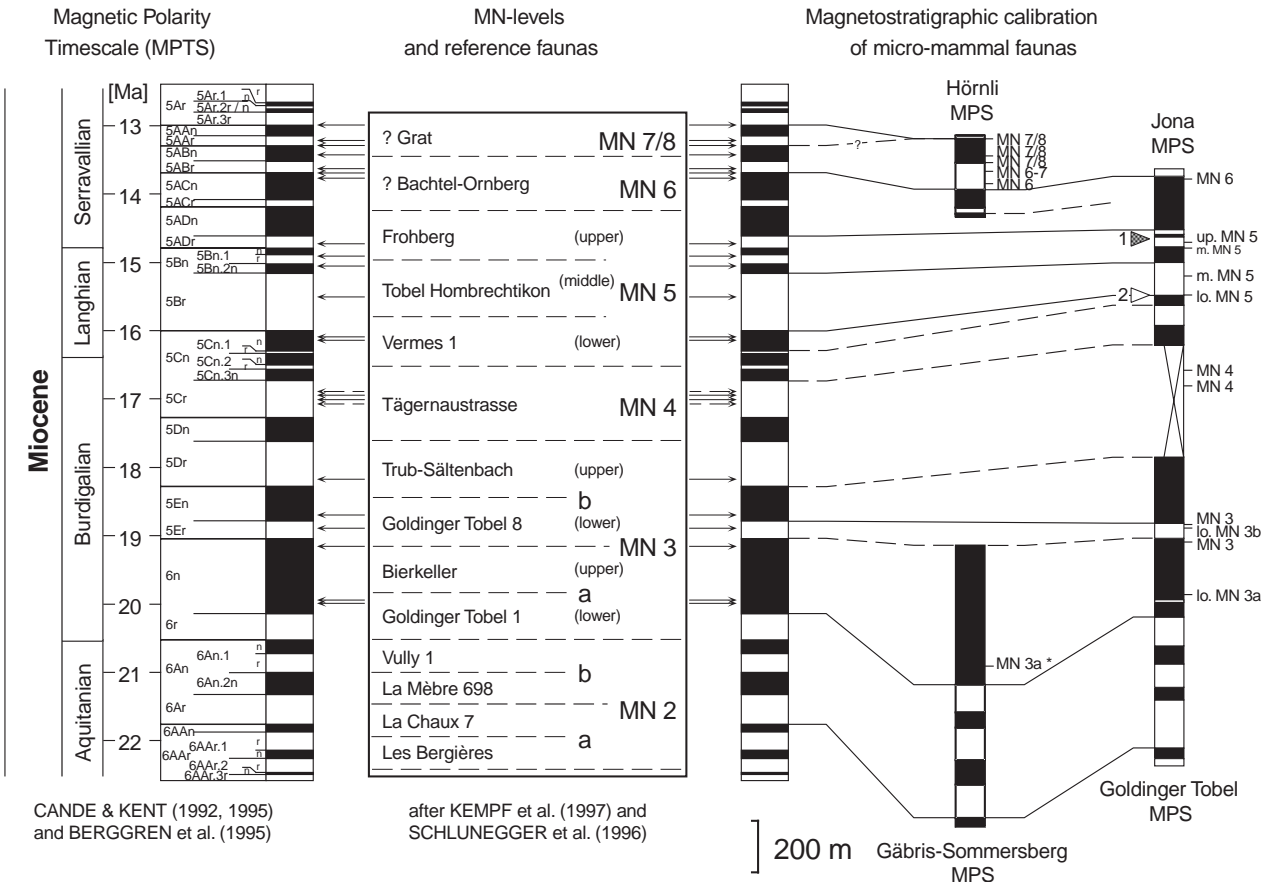
establish a detailed bio-chronostratigraphic framework (Burbank et al. 1992: two sections; Schlunegger et al. 1996: eight sections; Kempf et al. 1997: four sections). The magnetostratigraphic correlation of the sections from the eastern Swiss Molasse Basin (Gäbris-Sommersberg, Goldinger Tobel, Hörnli, and Jona section) is given in Fig. 4. These four sections, together with two sections from central Switzerland (see details in Kempf et al. 1997), were used to calibrate micro-mammal faunas of MN 3 to MN 7/8 (21–13 Ma; Fig. 4). The magnetic polarity stratigraphy (MPS) of the Gäbris-Sommersberg section (USM II–III) is interpreted to encompass chrons 6AA_n–6_n of the global Magnetic Polarity Timescale (MPTS; Cande and Kent 1992, 1995) and represents the time interval between 22 and 19 Ma. This indicates that terrestrial USM deposition persisted in eastern Switzerland until ca. 19 Ma, whereas marine sedimentation (OMM) had already started in central Switzerland at ca. 20 Ma (Berger 1985; Schlunegger et al. 1996). The MPS of the Goldinger Tobel section (USM II to OSM I) is interpreted to comprise chrons 6AA_r.1_r–5En, covering the time interval from ca. 22 to 18.3 Ma. The Jona MPS (OSM II) includes chrons 5C_n.3_n?–5AB_r covering a time span of ca. 16.5–13.5 Ma. The stratigraphically important Hüllstein marker horizon located within this

section (Fig. 2A,B; Bürgisser 1984) is assigned an age of ca. 16 Ma based on the MPS. The Hörnli MPS (OSM II) comprises chrons 5AD_n–5Ar.3_r? spanning the time period between ca. 14.5 and 13 Ma.

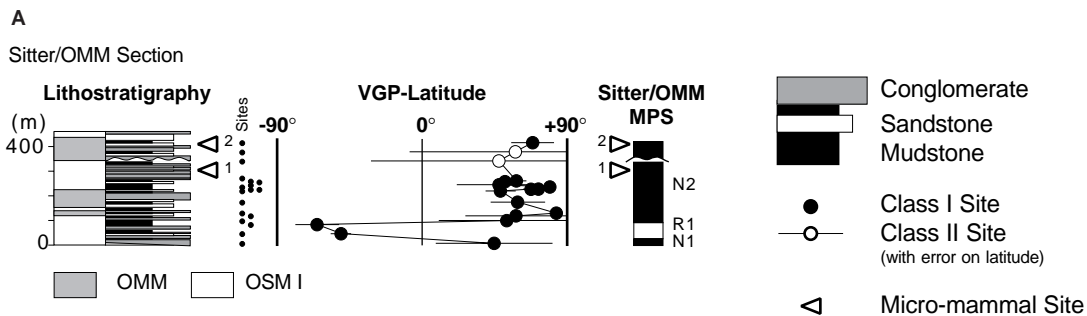
Magnetostratigraphic correlation based on micro-mammal faunas

The Sitter/OMM section shows an interfingering of marine (OMM) and continental (OSM I) deposits at the eastern margin of the Hörnli fan delta (Figs. 2A, 5A; Keller 1989). Three reversals were detected in this 450-m-thick section defined by two or more class-1 sites. Only the lowermost reversal (N1) is represented by a single class-1 site. Sample spacing is 20–25 m on average. The magnetostratigraphic section is constrained by two micro-mammal sites taken from

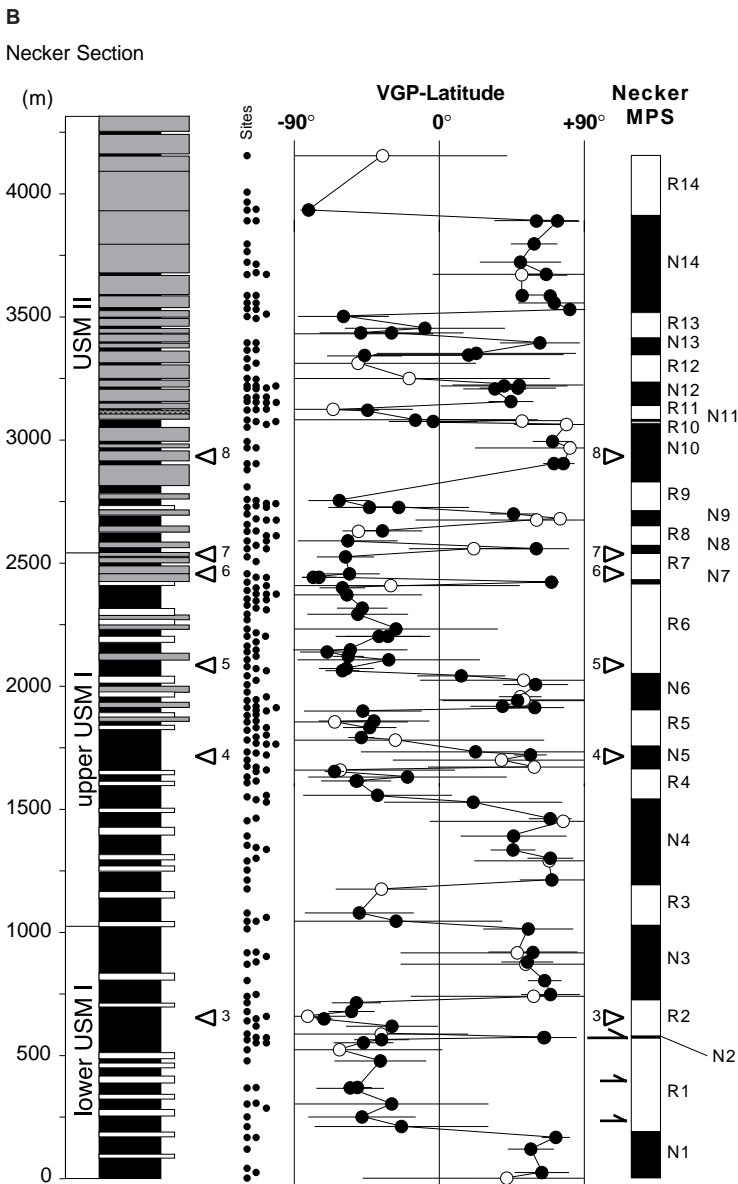
Fig. 4 Magnetostratigraphic calibration of micro-mammal faunas from the eastern Swiss Molasse Basin, modified after Kempf et al. (1997). The correlation of the individual magnetic polarity stratigraphy (MPS) including the micro-mamma faunas is constrained by the correlated Künsnacht bentonite (14.91 ± 0.09 Ma; Gubler et al. 1992) following Bolliger (1992, 1994). Additional sections from the central Swiss Molasse are not shown



1: Künsnacht bentonite (14.91 ± 0.09 Ma)
 2: Hüllstein marker horizon
 *) KÄLIN 1998 (pers. comm.)



Lithostratigraphy and Biostratigraphy after KELLER (1989)



A
Sitter/OMM Section
 KELLER (1989), KÄLIN (1997):
 1 Goldach-Martinsbrücke (Trub-Säitenbach/upper MN 3b)
 2 Sitter 418.5 m (Tägernastrasse/MN 4 or younger)#

B
Necker Section
 MöDDEN (pers. comm. 1994):
 3 OK-5 (MP 26 ± 1 zone)
 4 OK-1 (MP 28 ± 1 zone)

FREI (1979), ENGESSER (1990) (projected):
 5 Ebnat-Kappel (Fornant 6/up.MP 28)
 6 Wintersberg-Trempel (Küttigen or older/up.MP 29 or older)
 7 Krummenau-Thur (Brochene Fluh 53/up.MP 30)
 8 Krummenau-Umgehungsstrasse (Fornant 11/up.MN 1)

Keller (1989; Fig. 5). Site 1 (Goldach-Martinsbrücke), well correlatable from approximately 3–4 km further east to the section below the final marine transgression, contains a fauna of upper MN 3b (Kälin 1997), whereas the fauna of site 2 (Sitter 418.5 m) is of MN 4 or

younger (Fig. 5A; Keller 1989). Based on the calibration chart of Kempf et al. (1997), these two mammal sites allow the following correlation (Fig. 6): N2 is split into two segments and correlated to chrons 5En and 5Dn, N1 and R1 represent the top of chron 6n and

Fig. 5 A Magnetostratigraphy and micro-mammal faunas of the Sitter/OMM section. The stratigraphic column shows the interfingering of marine (OMM) and continental (OSM I) deposits. **B** Sedimentology, magnetostratigraphy and micro-mammal faunas of the Necker section (USM I–II). The reversals N1 and R1 are not used for correlation because of multiple thrusts with unknown displacement. Small filled dots indicate the stratigraphic position of sampling sites. Quoted error is the α_{-95} error on the VGP latitude. Class-I sites have three or more samples with Fisher (1953) $k > 10$. Class-II sites have unambiguous polarity, but $k < 10$

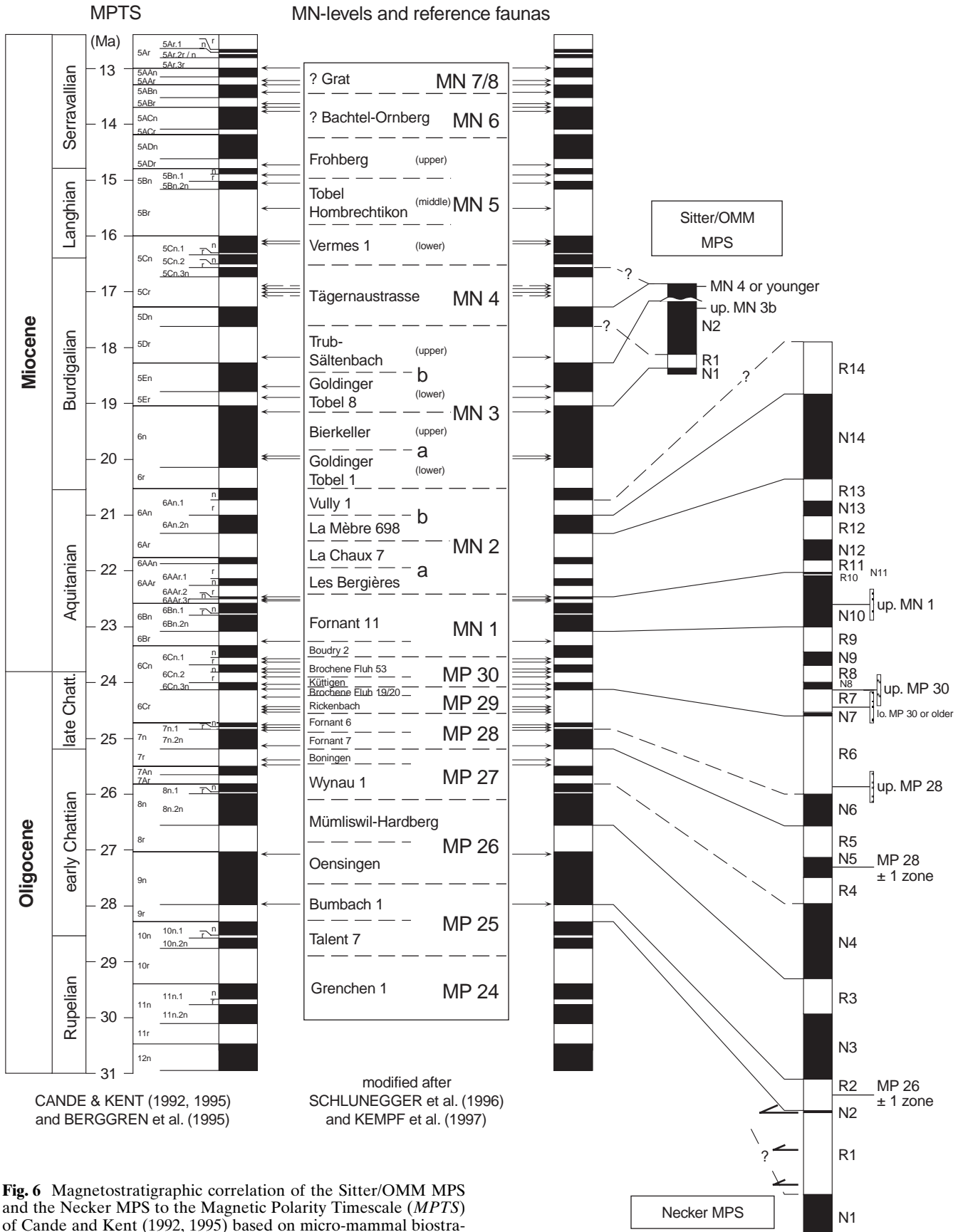


Fig. 6 Magnetostratigraphic correlation of the Sitter/OMM MPS and the Necker MPS to the Magnetic Polarity Timescale (MPTS) of Cande and Kent (1992, 1995) based on micro-mammal biostratigraphy (Frei 1979; Engesser 1990). An error bar (± 75 m) is added to the projected sites in the Necker section (see text)

chron 5Er, respectively, resulting in an erosional gap of ca. 0.5 Ma within the OMM (covering at least chron 5Dr). This correlation is justified by the evolutionary stage of the upper MN 3b fauna, which is placed near the base of Trub-Sältenbach and interpreted to be slightly older than the reference fauna (Kälin 1997; D. Kälin, pers. commun.). Given the faunal data, the theoretically possible correlation of N1–N2 to chron 5En to 5Dn is very problematic. Alternatively, the upper segment of N2 represents the normal chrons of 5Cn, because the fauna of site 2 may also be younger than MN 4. The last correlation would, however, require a strong increase of the sedimentation rate because approximately 500 m of sediment (Büchi 1950) are present between N2 and the Hüllistein marker horizon at 16 Ma (Fig. 4). The existence of an erosional gap within the OMM has already been suggested by Büchi (1956) based on biostratigraphic data. In a seismic study of the OMM of central Switzerland Schlunegger et al. (1997a) were able to identify magnetostratigraphically an erosional gap at the southern basin margin within chron 5Dr. Hence, a correlation of the top of N2 to chron 5Dn seems to be more reasonable and is thus used for further interpretations. As a consequence, the basal marine transgression of the OMM occurred ca. 1 Ma later than in central Switzerland and reveals, again, the heterochroneity of facies in the Swiss Molasse Basin (see Keller 1989 and Schlunegger et al. 1996 for justification). Nevertheless, other interpretations as mentioned above cannot completely be ruled out.

The ca. 4300-m-thick Necker section is located in the Kronberg thrust sheet of the Subalpine Molasse (Figs. 2A, 5B) and comprises most of the USM I–II. Two sites within the section contain micro-mammals (3 and 4 in Fig. 5B) representing the biozones MP 26 (± 1 zone) and MP 28 (± 1 zone). Four sites (5–8 in Fig. 5B) were projected from the Thur valley, approximately 4 km to the west, based on their stratigraphic position relative to the first appearance of crystalline clasts in the conglomerates which is supposed to be an isochronous reference level at the local scale (see also Fig. 9). The uncertainty of this reference level is estimated to ± 75 m at most, due to outcrop limitations in the Thur valley.

Good-to-excellent outcrop conditions in the Necker section allowed a sampling density for magnetostratigraphy of ca. 25 m in the lower 1500 m and less than 20 m between 1500 and 3500 m (Fig. 5B). Coarse-grained conglomerates prevented dense sampling in the uppermost part. The Necker section consists of 130 sites (76% class I) which define 28 magnetozones. The base of this section (N1 and R1) was probably affected by thrusting and repetition of strata. Therefore, these magnetozones were not used for magnetostratigraphic correlation (Fig. 6). Due to the high sampling density, we infer that all major chrons have been detected and are defined by two or more sites and by at least one class-I site. Only a few of the shorter magnetozones are

either defined by only a single class-I or class-II site (N7, R10, and N11). This assumption seems to be appropriate since the duration of individual channel belts are of the order of 10^4 – 10^5 years at most (Johnson et al. 1985; Miall 1991), whereas the duration of major magnetozones generally exceeds 10^5 years.

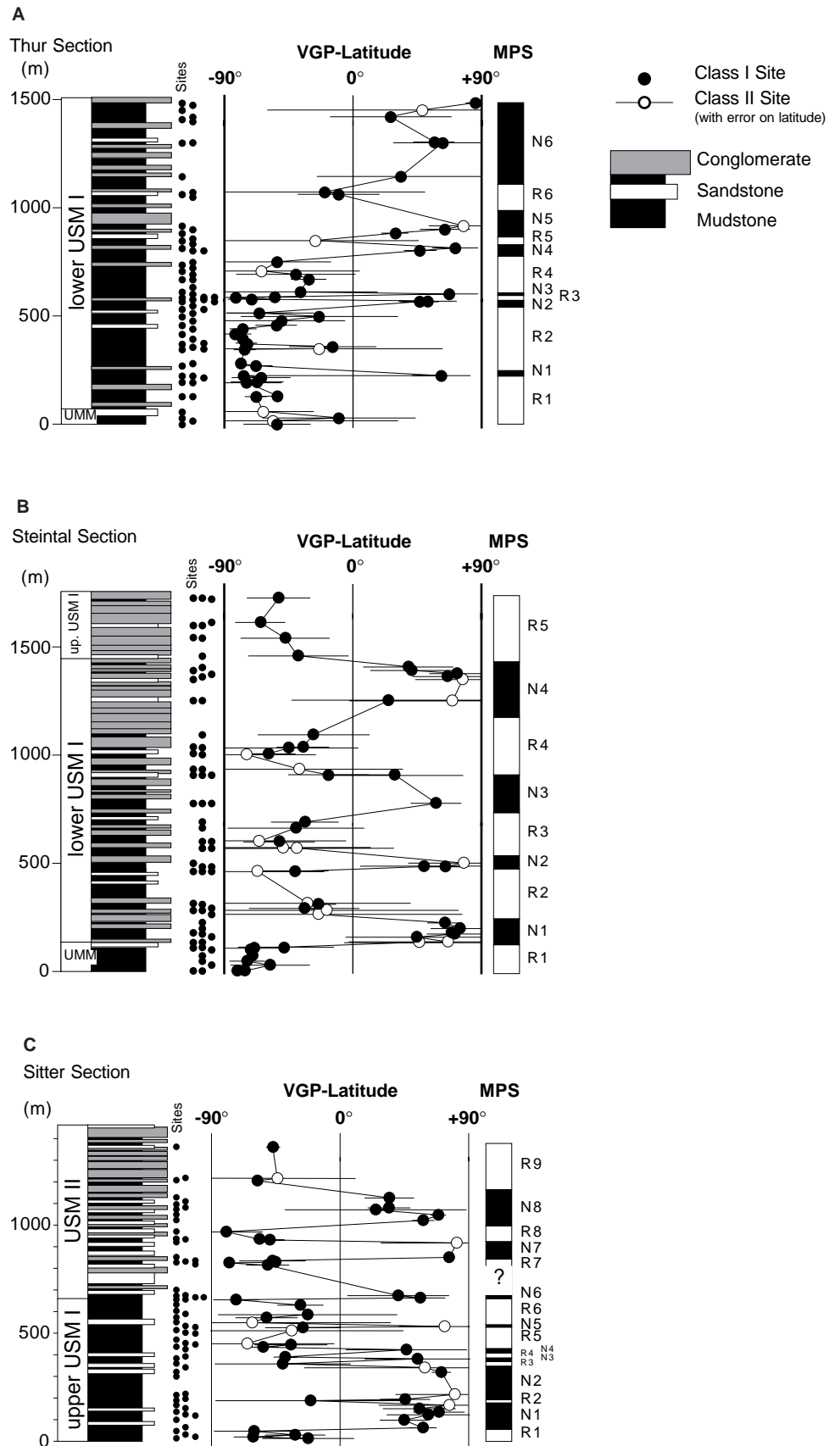
The projected micro-mammal faunas allow a good correlation of the magnetozones R6 to N10 to the MPTS (chrons 6Cr/?7n.1r to 6Bn.1n/6Bn.2n) within the estimated error (Fig. 6). Below R6, the correlation of the reversal patterns (N2–R5) is straightforward and further constrained by two mammal faunas (although less well defined). The upper part of the section (R10–R14) is correlated by the succession of normal and reversed polarities to chrons 6AAr.3r–6An.1r that very likely have all been detected within the continuously prograding alluvial fan system (coarsening- and thickening-upward sequence; Kempf 1998). No significant erosion of strata is recognized. Alternative correlations, e.g., N14 to chron 6n as suggested by the “long” normal period, need to explain many missing reversals. Only the top (R14) is poorly defined and another possible correlation may include chrons 6An.1n and 6r. This would, however, necessitate a major decrease in the sedimentation rate which appears inconsistent with the very proximal situation of the fan (Kempf 1998). Hence, we correlate the Necker section with the chrons 10n.1n to 6An.1r (N2–R14) representing the time period between ca. 28.3 and 20.7 Ma (Fig. 6). Only a few of the very short subchrons ($\leq 10^5$ a) are either defined by only one class-I or class-II site (N7, R10, and N11) or were missed (8n.1r, ? 7n.1r, ? 7n.1n and 6Bn.1r).

Magnetostratigraphic correlation based on petrography

No micro-mammal faunas are present in the Thur, Steintal, and Sitter sections (Figs. 2A, 7). Their magnetostratigraphic correlation is therefore based on characteristic heavy minerals or key clasts in the conglomerates in comparison with well-constrained sections (see below).

The Thur section is located in the southernmost Speer thrust sheet and comprises the uppermost 70 m of UMM and 1400 m of lower USM I (Figs. 2A, 7A). Sample spacing is 20–25 m with two gaps of ca. 100 m in the upper part of the section. The Thur MPS consists of 12 reversals defined by 50 sites (86% class I). The 1800-m-thick Steintal section, located in the Schorhüttenberg thrust sheet, is also composed of the uppermost UMM (130 m) and USM I (Figs. 2A, 7B). Sampling density is 30 m on average; however, some larger gaps of more than 100 m occur within the section. Nine reversals have been defined by 51 sites (73% class I). The deposits of the Thur, Steintal, and lower Necker section (USM I) are characterized by the key heavy mineral spinel showing a peak of $\geq 20\%$ and a drop thereafter (Frei 1979). This spinel peak provides a good correla-

Fig. 7 Sedimentology and magnetostratigraphy of the **A** Thur section, **B** Steintal section and **C** Sitter section



tion among these sections (Figs. 8, 9). Thus, we correlate magnetozones R6 (Thur MPS; Fig. 7A) and R4 (Steintal MPS; Fig. 7B) with R2 (Necker MPS; Fig. 6), which is correlated to chron 9r at ca. 28 Ma (Fig. 8). Consequently, the Thur MPS is interpreted to correlate to chrons 12r–9n of the MPTS, representing an age of ca. 31.5–27 Ma (Fig. 8). The relatively short magnetozones N1, N2, and N3 (compared with the MPTS), can be explained partly by erosion through scouring channels or outcrop gaps. The correlation of the Steintal MPS is more problematic because of two larger sampling gaps in N3 and R2 (Fig. 7B) where short subchrons, such as 11n.2n, 11n.1r, and 10n.1r, may have been missed. If so, the Steintal MPS correlates with chrons 12r–8r covering a time period of ca. 31–26.5 Ma (Fig. 8). This correlation is supported by the evolution of the spinel showing an initial increase (in R2 of Thur and Steintal section) followed by a reduced abundance and the peak at ca. 28 Ma (Fig. 9). With these correlations, the regression of the UMM sea started much earlier in the eastern Swiss Molasse Basin (Thur section: 31.5 Ma; Steintal section: 31 Ma) than in central Switzerland (30 Ma; Schlunegger et al. 1996). This reinforces the interpreted heterochrony of the lithostratigraphic units of the Molasse, as proposed by Keller (1989), and implies the transport of large amounts of debris into the basin causing the coastline to retreat.

The 1400-m-thick Sitter section, located in the northernmost Gäbris thrust sheet, represents the more distal parts of the USM I–II (Figs. 2A, 7C). Sample spacing is 20–25 m on average in the lower 700 m, and 40 m between 700 and 1400 m including two larger outcrop gaps. Seventeen magnetozones (R1–R9) were defined by at least two sites and include at least one class-I site. There are, however, five single-point reversals, most of them defined by class-I sites (Fig. 7C). Due to a large sampling gap between N6 and R7, the Sitter MPS was interrupted. A very important petrographic marker is present, i.e., the occurrence of crystalline clasts (gneiss) in the conglomerates (see details in Fig. 9). This petrographic change is interpreted as the onset of a new dispersal system and therefore considered as isochronous with respect to the paleomagnetic resolution. In the Necker (R8; Fig. 6) and in the Sitter section (above N6; Fig. 7C) this marker is tied to chron 6Cn.1r (Fig. 8). The base of the Sitter MPS (R1) is correlated to chron 8r because its very low spinel content does not allow a correlation with chron 9r. The correlation between chrons 8r and 6Cn.1r is drawn tentatively due to the predominance of reversed and normal polarities (Fig. 8). N8 is correlated with the normal chrons of 6Bn; the upper limit may correspond to the reversals of chron 6AAr. Based on the petrography and on the reversal pattern we correlate the Sitter section to chrons 8r to 6AAr.1r (ca. 27–22 Ma; Fig. 8). The resulting sedimentation rates (compacted) are 0.2 mm/a for the distal USM I and >0.5 mm/a for the proximal USM II.

Evolution of dispersal systems

The facies relationships at the southern basin margin were delineated through detailed mapping of the different depositional systems being heterochronous in terms of the magnetic chronologies (Fig. 10). Five major dispersal systems were recognized in the study area and were defined primarily by their characteristic suite of heavy minerals, but also by the clast composition of the conglomerates (Figs. 9, 11A). The geometry and spatial distribution of the individual dispersal systems is given by paleocurrent measurements (Figs. 2B, 11B).

The oldest system, active between ca. 31.5 and 24 Ma, is referred to as Speer dispersal system (Figs. 9, 11A). It is supplied mainly by the Speer alluvial fan with lesser contribution by the minor Stockberg alluvial fan, a few kilometers to the east (Figs. 2B, 10; Habicht 1945a, 1945b; Frei 1979). The conglomerates of both alluvial fans are composed of sedimentary clasts derived from Flysch and Austroalpine nappes (Renz 1937a). The sandstones are characterized by a high garnet content (Kempf 1998) and a suite of five heavy minerals, particularly zircon and spinel at the base, and zircon and apatite higher up (Fig. 9). The Speer and Stockberg fans revealed a cone-shaped geometry, indicating a transverse drainage that prograded into the basin. Farther north the drainage pattern changed into a basin-axial orientation with a paleoflow toward the northeast (Figs. 2B, 10B). Fan progradation resulted in an increasing sedimentation rate from <0.3 mm/a to >0.5 mm/a between 31.5 and 25 Ma (Fig. 11B).

The Speer system is succeeded by the more complex Kronberg-Gäbris dispersal system fed by three alluvial fan systems (Figs. 10, 11A; Renz 1937a, 1937b; Habicht 1945a, 1945b; Berli 1985): The Kronberg alluvial fan (24–21 Ma) consists of a transverse alluvial megafan and an axial conglomerate channel-belt depositional system. The Gäbris alluvial fan (23–20 Ma) is represented by a distal conglomerate channel-belt depositional system, and the locally sourced Sommersberg fan (20–19 Ma) developed as bajada depositional system. Between 24–20 Ma, the apex of these alluvial fans shifted 20–35 km in northeasterly direction (Figs. 2B, 10B). The conglomerates of the Kronberg and Gäbris alluvial fans are characterized by the occurrence of felsic crystalline clasts (up to 20%) in addition to sedimentary clasts (Fig. 9) derived from the crystalline core of the Austroalpine nappes according to Renz (1937a) and Habicht (1945a). The crystalline clasts are the major source of the key heavy mineral apatite in the sandstones (Fig. 9; Füchtbauer 1964). Although occurring at slightly different times, the substitution of apatite by epidote took place in the youngest deposits of both fans, where the first occurrence of greenschist and basic crystalline clasts in the conglomerates (<4%) is also recorded (Fig. 9; Habicht 1945a; Hofmann 1957).

These distinctive clasts are interpreted to have been derived from Penninic ophiolites and are the major

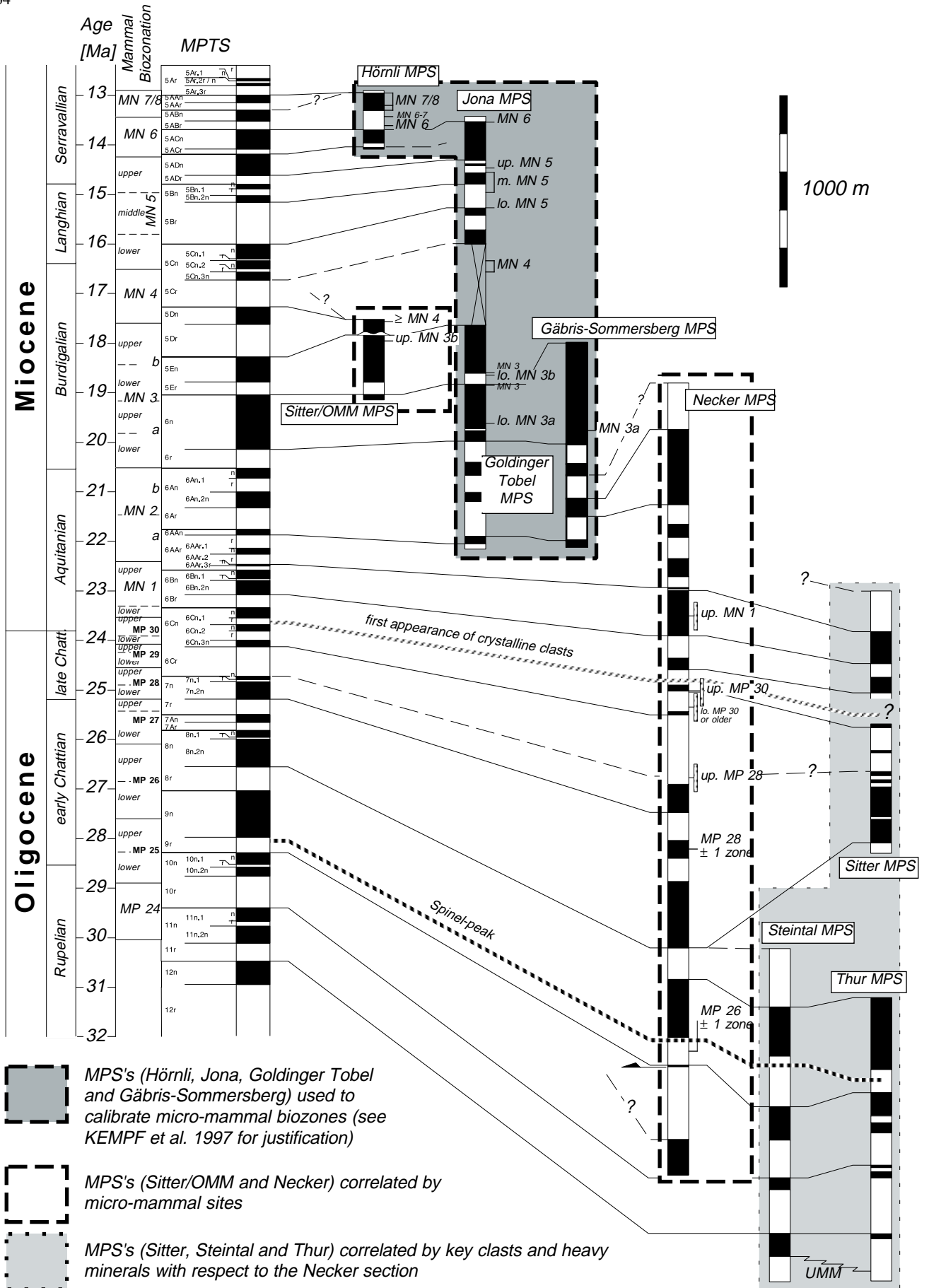


Fig. 8 Correlation of all magnetostratigraphic sections to the Magnetic Polarity Timescale (MPTS). Simplified mammal biozonation after Schlunegger et al. (1996) and Kempf et al. (1997). For discussion see text

source for epidote (Renz 1937b; Füchtbauer 1964; Dietrich 1969). Another source for epidote is crystalline clasts (gneisses and granites) associated with the greenschists (Füchtbauer 1964). Thus, it appears that the catchment area of both fans evolved differently through time. Penninic crystalline units were eroded at ca. 21 Ma in the west and around 20 Ma in the east. This is due either to differential uplift of Penninic units in the hinterland, or to a different lateral (southward) extension of the catchment areas.

The presence of two petrographically very similar alluvial fans (Renz 1937b; Hofmann 1957) is indicated by the cone-shaped geometries of the Kronberg (western tributary) and Gäbris fan (eastern tributary), as well as by mapping of the zones of maximum accumulation of coarse conglomerates (Figs. 2B, 10B; Ludwig et al. 1949). Both fans, ca. 10–15 km apart, were active between 23 and 21 Ma and prograded in northern direction (Fig. 10A). Sedimentation rates increased greatly during this period, from 0.3 to >1.0 mm/a in the Kronberg fan and from 0.3 to ca. 0.5 mm/a in the Gäbris fan (Fig. 11B). Bajadas developed on the flanks and on top of the Kronberg fan (Fig. 10). The clast composition of these deposits is typically dominated by (Ultrahelvetic and North-penninic) Flysch clasts (Fig. 9; Gasser 1967; Woletz 1967). Forming on the eastern flank and succeeding the Gäbris fan (Fig. 10B), the Sommersberg fan shows a similar petrographic composition to the bajadas encroaching the Kronberg fan implying the same local source from the frontal range of the Alps (Fig. 9). Nummulitic limestone clasts derived from the Eocene Helvetic Einsiedeln, Bürgen, and Klimsenhorn formations (Yprésien-Lutétien; Menkveld-Gfeller 1997) occur for the first time (Leupold et al. 1942; Tanner 1944; U. Menkveld-Gfeller, pers. commun.). The Gäbris-Sommersberg section contains individual beds of Granitic Sandstone in the Gäbris fan derived from the Höhrone and Napf dispersal systems (see below; Fig. 9; Renz 1937b; Füchtbauer 1964), suggesting the interference of the different dispersal systems without mixing.

The Höhrone and Napf dispersal systems (Fig. 11A) did not originate in the study area but deliver large amounts of debris through an axial drainage from SW into the region (Fig. 2B; Hofmann 1957; Schlanke 1974; Schlunegger et al. 1997b). These systems had been active between 24 and 14.5 Ma (Matter 1964; Keller 1989; Schlunegger et al. 1997b) and are characterized by the key heavy minerals zircon, apatite (Höhrone: Kleiber 1937; Schlanke 1974), and epidote (Fig. 9; Napf: Füchtbauer 1964; Matter 1964). In the study area

this axial drainage was temporally limited to the time interval between 24 and 20 Ma (Fig. 11A), and sedimentation rates were nearly constant between 0.2 and 0.3 mm/a (Fig. 11B). The heavy mineral data suggest no mixing of this axial drainage with the radial Kronberg-Gäbris dispersal system (Figs. 9, 11A).

The Hörnli dispersal system is the youngest system of the eastern Swiss Molasse Basin and was active during ca. 20–13 Ma (Fig. 11A; Kempf et al. 1997). The heavy mineral composition of this system is generally dominated by epidote except at the base, where apatite, zircon, and rutile are major components (Fig. 9; Füchtbauer 1964). The clast composition is very similar to the Kronberg-Gäbris dispersal system, consisting of crystalline clasts from Austroalpine and Penninic nappes (generally <20%, decreasing toward the top) and sedimentary clasts from Austroalpine, Penninic, and Helvetic nappes (Tanner 1944; Büchi 1950; Büchi and Welti 1951). The apex of the Hörnli alluvial fan is situated 30 km west of the Sommersberg fan apex (Fig. 2B). Fan progradation to the north started slowly and increased shortly after deposition of the Hüllstein marker bed at 16 Ma (Fig. 10A; Bürgisser 1980, 1981). Sedimentation rates of 0.2 to >0.3 mm/a were low when compared with those of the Speer and Kronberg-Gäbris fans.

Large amounts of debris were delivered into the OMM sea by the large Hörnli fan delta between 19 and 17 Ma (Büchi 1950; Habicht 1987), as reflected in the predominance of epidote in the terrestrial deposits (Figs. 6, 10B). The heavy mineral association of the intercalated marine sandstones is characterized by a high amount of apatite typical of the OMM of eastern Switzerland (Figs. 5A, 9; Allen et al. 1985). The different heavy mineral composition at the base of the Hörnli dispersal system between 20 and 19.5 Ma (Goldinger Tobel section; Fig. 9) possibly represents the last influence of an apatite-dominated hinterland of the former Kronberg-Gäbris dispersal system. Other petrographic changes were recognized at 16 and 14 Ma in the sections of Jona and Hörnli, including a decreasing epidote content and an increase of a suite of accessory heavy minerals of predominantly metamorphic origin. The increase of staurolite indicates downcutting into metamorphic Penninic units, whereas topaz and andalusite suggest an influence from the Bohemian Massif (Fig. 9; Hofmann 1976; Allen et al. 1985).

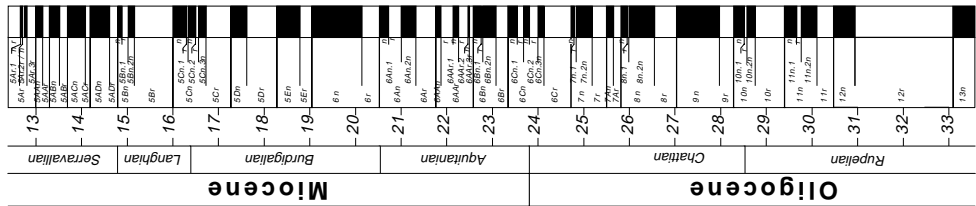
Discussion

Tectonic evolution of the southern basin margin

31.5–24 Ma. Initial stage: flysch nappe propagation

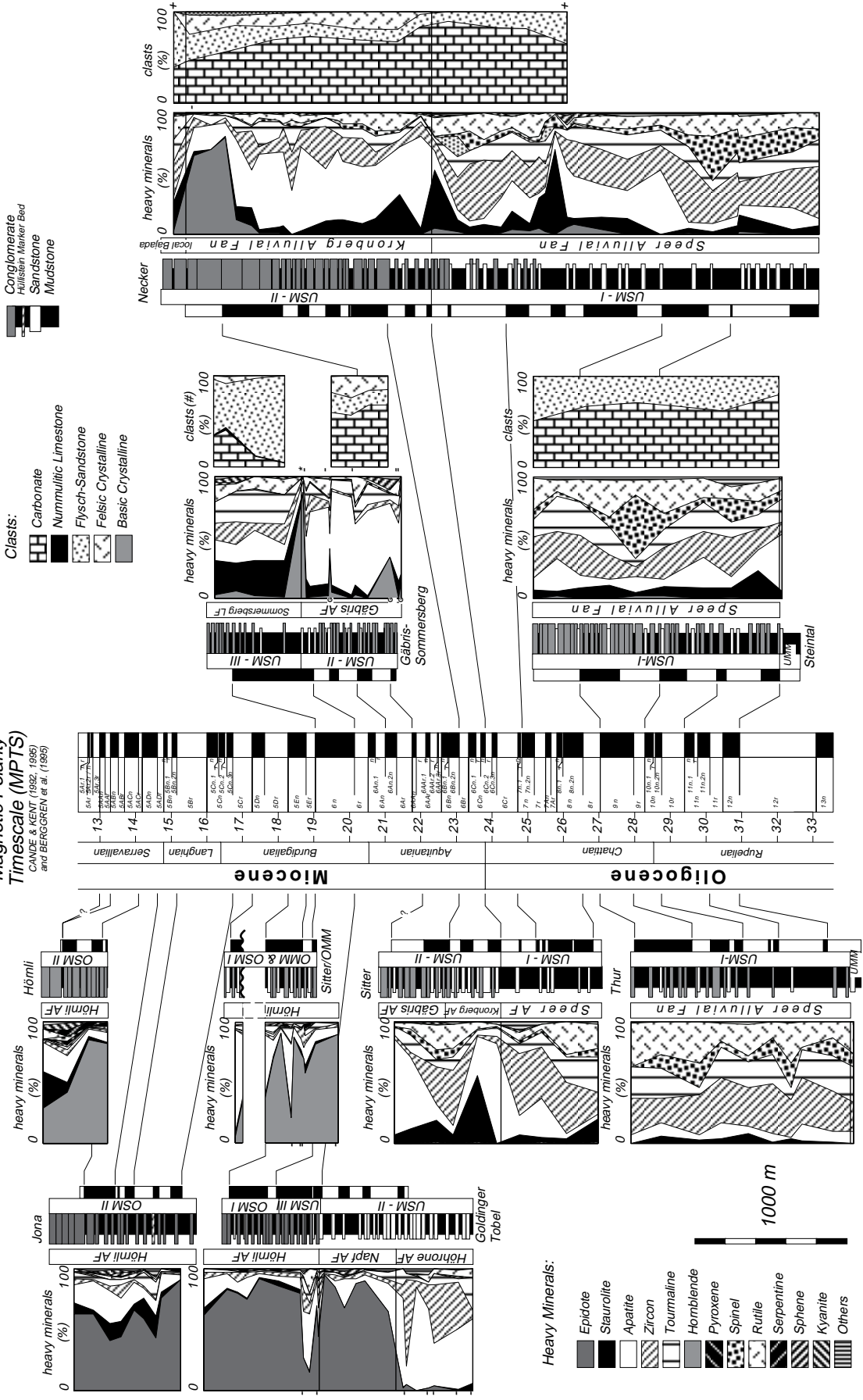
During deposition of the UMM, the northern margin of the narrow seaway in the study area (Diem 1986; Berger 1996) seemed to be fault controlled since major

Magnetic Polarity Timescale (MPTS)
 CANNON & KEAY (1992, 1995)
 and BERGGREN et al. (1985)



Clasts:
 Conglomerate
 Alluvial Marker Bed
 Sandstone
 Mudstone

Heavy Minerals:
 Carbonate
 Nummulitic Limestone
 Flysch-Crystalline
 Felsic Crystalline
 Basic Crystalline



Heavy Minerals:

- Epidote
- Staurolite
- Apatite
- Zircon
- Tourmaline
- Hornblende
- Pyroxene
- Spinel
- Rutile
- Serpentine
- Sphene
- Kyanite
- Others

Fig. 9 Heavy mineral and clast composition of all studied sections and the relationship to the individual dispersal systems. Samples of Granitic Sandstone in the Gäbris-Sommersberg section are marked G. Additional petrographic data from Renz (1937b, #; Habicht 1945a, +; Hofmann (1957, *) and Füchtbauer (1964, -)

normal faults are present on seismic lines along the southern margin of the Plateau Molasse (Fig. 3A; Stäubli and Pfiffner 1991; Pfiffner et al. 1997a). Deposition of the lower USM I (31.5–27 Ma; Fig. 9) started with the northward prograding Speer alluvial fan. Its constant thickness in the Thur and Steintal sections over approximately 20 km in downcurrent direction and constant dip from base to top (Fig. 2A) suggest uniform subsidence during this initial stage of basin evolution (Fig. 12A,B). No sediments were recognized younger than ca. 27 Ma in both sections (Fig. 10A). Farther north, the sedimentation rate increased in the Necker section between 27 and 25.5 Ma from 0.4 to >0.5 mm/a (Fig. 11B). Moreover, the amount of Flysch clasts derived from the Alpine thrust front increased in the uppermost portion of the Steintal section at 27 Ma, as well as in the Necker section between 26 and 25 Ma (Fig. 9; Habicht 1945a). This can be explained by a phase of ongoing in-sequence thrusting of Flysch nappes between 27 and 25 Ma that encompasses the area of the Thur and Steintal sections. The tip of the wedge at 25 Ma was south of the Necker section (Fig. 12B). The advance rate of the Flysch nappes is roughly estimated to less than 3 cm/a considering our chronologies and the interpreted N–S extension of the lower USM-I deposits (Fig. 3A; Pfiffner et al. 1997a). Increasing sedimentation rates (Necker section; Fig. 11B) and a gradual decrease of the dip angle up-section (50–35°; Fig. 2A) suggest differential subsidence after 26 Ma, due to extension of the tectonic load caused by basinward transport of the orogenic wedge (see also Beaumont 1981; Sinclair et al. 1991). Hence, after 26 Ma, the basin became more wedge-shaped at the tip of the thrust front. Between 25.5 and 24 Ma the decreasing sedimentation rate (Necker section; Fig. 11B) reflects a time of relative tectonic quiescence in the wedge. A regional unconformity which developed during quiescence, as proposed by Schlunegger et al. (1997b) ca. 50 km farther west, has not been recognized at the thrust front during that time.

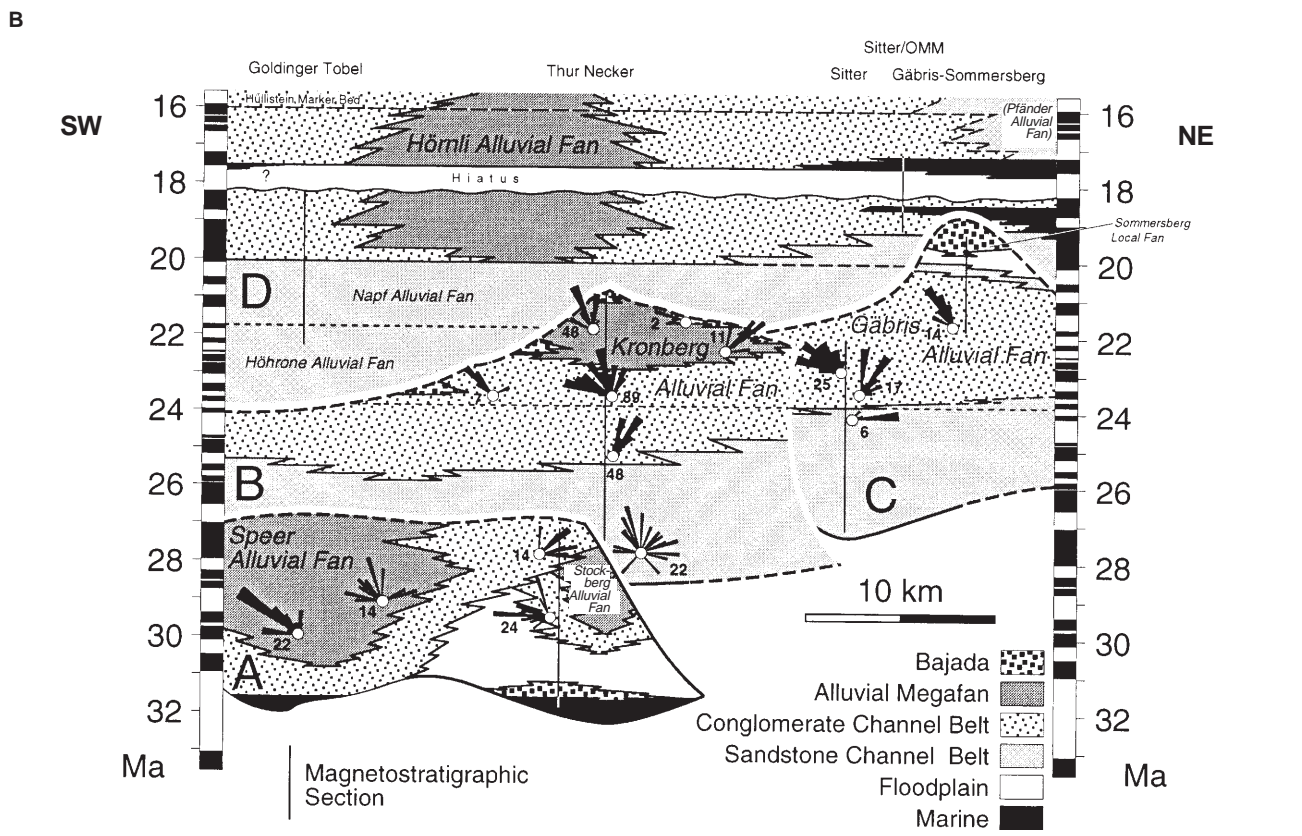
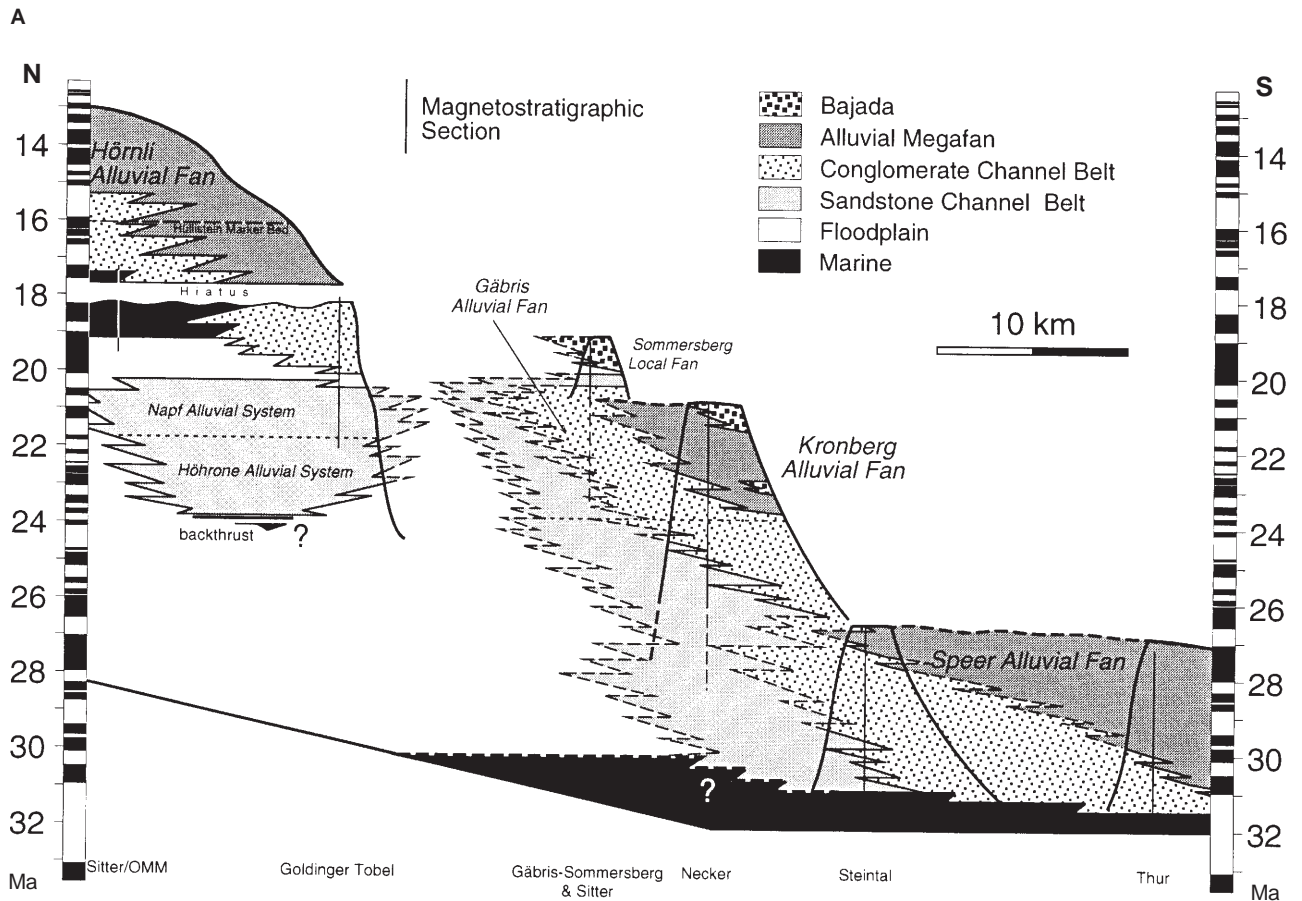
24–19 Ma. Second stage: Molasse accretion to wedge, initiation of triangle zone

At ca. 24 Ma older Molasse strata (USM I, 31.5–26.5 Ma) were incorporated into the Alpine orogenic wedge (Fig. 12C) as suggested by the following observations: the dip angle of USM-II deposits (ca. 24–21 Ma) decreases gradually from 35–20° up-section (Necker section; Fig. 2A), possibly due to further increase of the tectonic load, and the heavy mineral

composition changed abruptly. In contrast, the clast composition of the conglomerates remained unchanged until ca. 23.3 Ma, when the contribution of crystalline clasts increased to approximately 15% (Fig. 9). This discrepancy can best be explained by accretion of lower USM I to the orogenic wedge (Fig. 12C), such that reworking of these deposits contributed large amounts of sedimentary clasts to the newly formed crystalline-bearing Kronberg-Gäbris dispersal system and initially overprinted the crystalline influence (Fig. 9). As another significant consequence of the incorporation of Molasse deposits (USM I) to the orogenic wedge, the apex of the Speer alluvial fan was blocked off and the apex of the new Kronberg alluvial fan shifted ca. 20 km farther northeast (Fig. 2B). A second apex (Gäbris alluvial fan) developed at 23 Ma approximately 12 km farther northeast (Fig. 2B). As a result of thrust activity within the Subalpine Molasse, the whole drainage system migrated in a northeasterly direction.

At ca. 20 Ma more Molasse strata were accreted to the orogenic wedge (Fig. 12D). The changing clast composition of the conglomerates of the Sommersberg fan implies a normal unroofing of the thrust front and the underlying Molasse (USM II) strata: The base is composed mainly of thrust-front material (Flysch sandstones) towards the top, and the amount of clasts from USM I and II deposits increased (carbonates and crystalline up to 40%, Gäbris-Sommersberg section; Fig. 9). This second phase of accretion influenced the drainage system considerably: The Kronberg and Gäbris alluvial fans were abandoned at ca. 21 and 20 Ma, respectively, and the apex of the new local Sommersberg fan shifted ca. 8 km to the northeast (Fig. 2B).

The southern margin of the Plateau Molasse is made up of deposits from the axial dispersal systems of Höhrone and Napf (Büchi 1950) that are located north of the Kronberg-Gäbris dispersal system (Fig. 11A). The palinspastic restoration (Fig. 3B) reveals a limited N–S extent for the transverse Kronberg-Gäbris dispersal system (Fig. 12A). Its deposits were not reported north of the Höhrone/Napf dispersal systems (e.g., Büchi et al. 1965). Moreover, the distinct petrographic compositions of these three dispersal systems remained unaffected by each other throughout deposition (Fig. 9). This suggests a rapid change of the paleo-flow direction of the Gäbris alluvial fan from transverse to axial within a few kilometers and a drainage divide that prevented these systems from mixing. A possible cause therefore is the beginning of deformation of the triangle zone (Fig. 12D). Active thrusting beneath the drainage area resulted in a fluvial divide along strike separating the different dispersal systems between 24 and 20 Ma. The increased tectonic activity in northeasterly direction due to accretion and blind thrusting is also a possible reason for the northwestern shift of the apex of the predominant Hörnli fan at ca. 20 Ma. A major change in the catchment area is evidenced by the modified petrographic composition of the new Hörnli dispersal system (Fig. 9).



←

Fig. 10 A Chronological diagram (N–S) depicting the facies relationships of the southern margin of the eastern Swiss Molasse Basin. **B** Chronological diagram (SW–NE) delineating the facies relationships in four cross sections through the major thrust units of the Subalpine Molasse (A–C) and the upwarped margin of the Plateau Molasse (D). The four cross sections are arranged from south (A) to north (D) according to their palinspastically restored position. The magnetostratigraphic time frame is based on Fig. 8

19–13 Ma. Third stage: backthrusting of Plateau Molasse

The evolution of the Hörnli dispersal system started at ca. 20 Ma when sedimentation on the Gäbris alluvial fan had almost finished (Fig. 10). At that time the petrographic composition of both fans was very similar (Fig. 9). The sedimentation rate of the Hörnli dispersal system was low (0.2–0.3 mm/a) between 22 and 19 Ma but increased up to 0.5 mm/a thereafter (Fig. 11B). This coincides with the shift of the depocenter from the Subalpine realm to the area of the Plateau Molasse at 20–19 Ma when sedimentation in the Subalpine Molasse ended. A major erosional unconformity formed in the Plateau Molasse between ca. 18.3 and 17.8 Ma (Figs. 10, 11), as indicated by magneto- and biostratigraphic data from the eastern margin of the Hörnli fan delta (Sitter/OMM section; Figs. 5A, 8). Bolliger et al. (1995) described a low-angle unconformity between marine sandstones and underlying continental clastics at the southwestern flank of the Hörnli fan delta. The marine transgression is constrained by both biostratigraphic data (Bolliger et al. 1995) and magnetostratigraphy (Goldinger Tobel section; Fig. 8). An unconformity was also reported from the Molasse Basin approximately 50 km further west between 18.1 and 17.7 Ma (Schlunegger et al. 1997a, 1997b). This erosional phase possibly reflects uplift of the Subalpine Molasse (Fig. 12E) after accretion took place at around 20 Ma, probably in combination with a relative sea-level drop (Keller 1989). Moreover, the tilted sediments at the southern margin of the Plateau Molasse show a decrease in dip angle from ca. 50° at the base (SE) to less than 10° on top (NW; Goldinger Tobel and Jona section; Fig. 2A), suggesting continued syndepositional uplift in the area of the triangle zone and Subalpine Molasse. The uplift is probably related to backthrusting of the southern margin of the Plateau Molasse (Fig. 12E). Andalusite and topaz, two characteristic heavy minerals of the Bohemian Massif, but unknown from the Swiss Alpine hinterland (Büchi and Hofmann 1960; Hofmann 1976), occur rarely in the heavy mineral assemblage of the Jona section at ca. 15 Ma and in the Hörnli section at 13 Ma (<2% in “others”; Fig. 9). These heavy minerals are only reported from the so-called Muschelsandsteine (OMM) of the northern Molasse Basin, transported by strong basin-axial tidal currents (Allen et al. 1985). Although lacking proof by heavy mineral analyses, similar sandstones also appear

to have been deposited at the southern basin margin. Nevertheless, these sandstones are a possible source for andalusite and topaz in the Hörnli alluvial fan and thus suggest that exhumation and subsequent erosion of the southern margin of the Plateau Molasse started at around 15 Ma, probably due to backthrusting. The occurrence of andalusite and topaz in different stratigraphic levels of the Hörnli alluvial fan (at 15 and 13 Ma) suggests uplift, erosion, and recycling of marine sandstones from the flanks of the Hörnli fan delta at different times.

Molasse Basin evolution and Alpine tectonics

The tectono-stratigraphic evolution at the Alpine thrust front is related to tectonic movements within the Alpine orogen on a larger scale. Enhanced activity at the thrust front and marked changes in the catchment area of the dispersal systems represent major phases of tectonic activity in the Alps. Based on our magnetostratigraphic data from the eastern Swiss Molasse Basin, we propose the following timing of tectonic phases:

1. At 31.5 Ma alluvial sedimentation started with the formation of the large Speer alluvial fan in the southwestern part of the study area (Figs. 2B, 12A). The high sediment input is a response to exhumation of the southern Central Alps (Pfiffner and Hitz 1997), which is linked to backthrusting movements along the Insubric Line associated with synmagmatic vertical movements during the Bergell intrusion at 32–30 Ma (Schmid et al. 1989, 1996; Blanckenburg 1992). In addition, northward thrusting took place within the Helvetic nappes (initiation of Glarus Thrust, Calanda phase of Milnes and Pfiffner 1977, 1980; Pfiffner 1985, 1986). By that time Austroalpine nappes had been emplaced onto the Penninic units and covered large areas of the Alpine realm, and Penninic Flysch nappes formed the thrust front (Pfiffner 1986).
2. Prograding Flysch nappes buried the proximal Molasse at ca. 27–26 Ma (Fig. 12B) and led to an increasing amount of Flysch clasts in the more distal area of the Speer alluvial fan and non-deposition on the fan itself (Figs. 9, 10A). This northward propagation of the orogenic wedge coincided with movements along the Glarus Thrust (Schmid 1975; Calanda phase of Milnes and Pfiffner 1977, 1980; Pfiffner 1985, 1986) and ongoing backthrusting movements along the Insubric Line (32–19 Ma; Hurford 1986; Schmid et al. 1987, 1997; Zingg and Hunziker 1990). Between 25.5 and 24 Ma sedimentation rates decreased from >0.6 to 0.4 mm/a (Necker section; Fig. 11B) and coincided with a major unconformity recognized in the central Swiss Molasse Basin approximately 50 km further west (Schlunegger et al. 1997b), but not in the study area. The decrease in sediment accumulation may reflect a first phase of reduced tectonic activity.

Fig. 11 Chronostratigraphic schematic cross section (N–S) of the southern margin of the eastern Swiss Molasse Basin (based on Fig. 10A) showing **A** the distribution of the individual dispersal and drainage systems and **B** the sedimentation rates (compacted)

3. Accretion of Molasse deposits to the orogenic wedge is interpreted to have occurred at ca. 24 and 20 Ma (Fig. 12C,D; refer to Schlunegger et al. 1997b who also claimed accretion of earlier deposited Molasse strata to the orogenic wedge between 23 and 21.5 Ma in central Switzerland). This phase of Molasse accretion coincided with enhanced uplift of the central Southern Alps along the Insubric Line after 26 Ma due to rapid cooling and exhumation (>10 km vertical uplift in the Bergell area; Hurford 1986; Giger and Hurford 1989; Zingg and Hunziker 1990). Moreover, continued out-of-sequence thrusting along the Glarus Thrust led to a passive northward transport of deformed Helvetic units (Ruchi phase of Milnes and Pfiffner 1977, 1980; Pfiffner 1986), probably in combination with uplift of the eastern Aar massif at ca. 20 Ma (Pfiffner et al. 1997b). Simultaneously, the petrographic composition of the Molasse deposits changed markedly and imply major changes in the catchment area: At ca. 24 Ma basement units of the Austroalpine realm became initially eroded, and at ca. 21 Ma Penninic basement was eroded as indicated by ophiolitic clasts in the Molasse (Dietrich 1969). Contrasting petrographic spectra (Fig. 9) point to a fluvial divide separating the Höhrone/Napf and Kronberg-Gäbris dispersal systems between 24 and 20 Ma (Fig. 12D). Migration of the fan heads towards northeast between 24 and 20 Ma was probably caused by the shift of active Molasse thrusting in the same direction. Finally, the main drainage migrated back to the west and the most recent Hörnli alluvial fan became established.
4. An erosional unconformity is evident around 18 Ma (Fig. 10). By that time backthrusting along the Insubric Line (Hurford 1986; Schmid et al. 1989; Zingg and Hunziker 1990) as well as movements along the Glarus Thrust (Pfiffner 1986; Pfiffner et al. 1997b) had been finished. According to Schlunegger et al. (1997b) this basin-wide erosional unconformity was produced by backthrusting of the southern Plateau Molasse due to the ongoing formation of the triangle zone.
5. Backthrusting of the southern margin of the Plateau Molasse resulted in progressive rotation of the deposits, which gradually flatten from base (S) to top (N; Fig. 2A). The youngest deformed strata, ca. 15–14 Ma in age, mark the end of thrusting. Reworking of OMM sandstones is suggested at 15 and 13 Ma by the occurrence of andalusite and topaz in the heavy mineral assemblage. Sedimentation rates (Fig. 11B) increase at 15–13 Ma indicating

enhanced exhumation and subsequent erosion possibly due to backthrusting. The time interval of backthrusting of the Plateau Molasse postdates movements along the Insubric Line (Hurford 1986; Schmid et al. 1996, 1997) and is in good agreement with Schlunegger et al. (1997b) who argued that backthrusting is associated by underplating and exhumation of the central Aar massif due to indentation of the Adriatic lower crust (Michalski and Soom 1990; Pfiffner et al. 1997b).

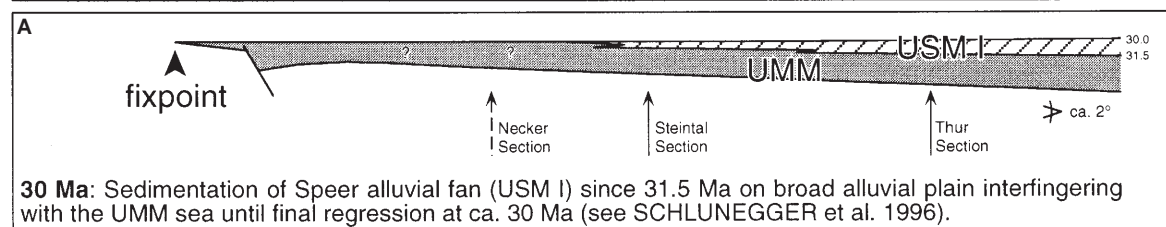
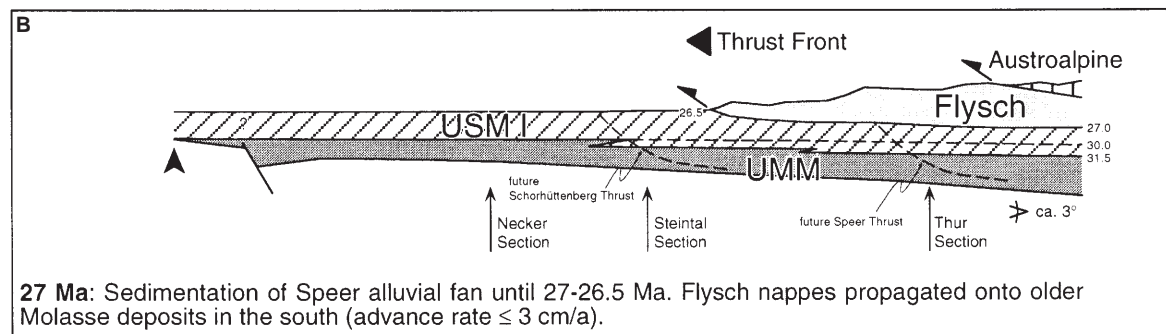
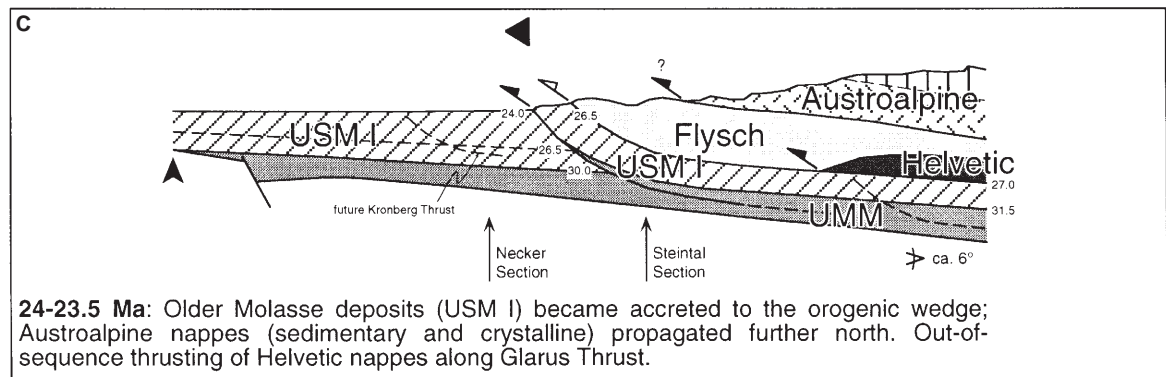
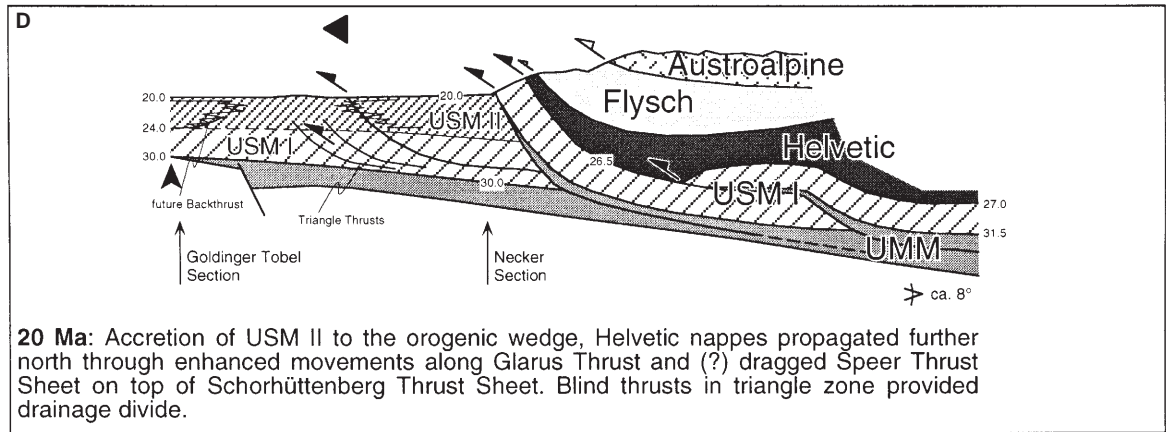
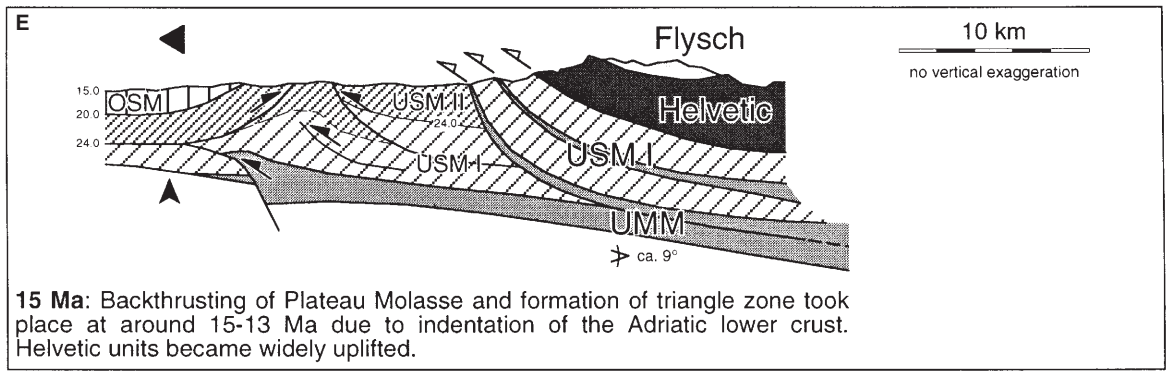
Conclusion

High-resolution magnetostratigraphy of nine sections, in combination with mammal biostratigraphy, provides a very detailed chronology for the Molasse stratigraphy at the southern margin of the North Alpine Foreland Basin. This allows precise dating of the lateral and vertical depositional evolution, sedimentation rates, and insights into the timing of tectonic processes that control the stratigraphic evolution.

Formation of petrographically different dispersal systems document the denudation history of the Alps. They were identified and defined by characteristic heavy mineral and clast assemblages which mimic the composition of their former catchment areas. Changes in the petrographic composition are therefore caused by modification of the catchment areas.

The thrust front was strongly modified in Late Oligocene to Middle Miocene times during phases of enhanced tectonic activity in the orogen leading to the growth of three prograding coarsening- and thickening-upward sequences of alluvial deposits. Propagation of the entire orogenic wedge initially started around 27–26 Ma probably in relation to uplift and exhumation of the southern Central Swiss Alps due to backthrusting along the Insubric Line between 32 and 26 Ma and by movements along the Glarus thrust of the eastern Swiss Alps. Accretion of Molasse deposits to the orogenic wedge took place in a second phase at ca. 24 and 20 Ma. This coincided with another period of rapid cooling, denudation, and inferred rock uplift of the Central Swiss Alps along the Insubric Line after 26 Ma and continued out-of-sequence thrusting movements along the Glarus Thrust. Backthrusting of the proximal foreland probably occurred thereafter and was synchronous with uplift of the central Aar massif in the course of underplating of the lower Adriatic crust.

Thrusting near the deformation front and the geometry of the thrust sheets themselves are also the most likely reasons for migration of alluvial fans. The different alluvial fan heads shifted through time from the southwest (Speer-Stockberg, 31.5–24 Ma) towards the northeast (Kronberg, 24–21 Ma; Gäbris, 23–20 Ma; Sommersberg, 20–19 Ma) and then back towards the northwest (Hörnli, 20–13 Ma). A possible reason for this migration was accretion of Molasse strata to the orogenic wedge that forced abandonment of the former



←
Fig. 12A–E Tectonic evolution in five steps from 30–15 Ma. *Full arrows* indicate active thrusting, *open arrows* depict no or only minor thrusting. See text for discussion

fan heads; hence, blocking of the drainage system at the thrust front demanded a lateral escape of the feeding rivers in four steps between 31.5 and 19 Ma. This tectonically induced shifting is also reflected in the structure of the eastern Swiss Molasse: Different thrust sheets taper out laterally and are displaced from southwest to northeast (Fig. 3).

Acknowledgements We thank F. Schlunegger (University of Jena) and O.A. Pfiffner (University of Bern) for fruitful discussions. Special thanks go to P. Strunck (University of Bern) for discussion and field support. The help of S. Burns (University of Bern) with the English is kindly acknowledged. We also thank H.-P. Bärtschi for technical assistance and H. Haas for the separation of heavy minerals. S. Lund and S. Henyey (University of Southern California) provided much appreciated technical assistance and advice with the paleomagnetic sample processing. The constructive reviews by J.-P. Berger and A. Wetzel improved the manuscript and are kindly acknowledged. This paper is part of O. Kempf's PhD thesis and was financially supported by the Swiss National Science Foundation (grant nos. 20-42890.95 and 20-50495.97).

References

- Allen PA, Mange-Rajetzky M, Matter A, Homewood P (1985) Dynamic palaeogeography of the open Burdigalian seaway, Swiss Molasse basin. *Eclogae Geol Helv* 78:351–381
- Beaumont C (1981) Foreland basins. *Geophys J R Astr Soc* 65:291–329
- Berger J-P (1985) La transgression de la molasse marine supérieure (OMM) en Suisse occidentale. *Münchner Geowiss Abh (A)*, Verlag Friedrich Pfeil, München, pp 1–208
- Berger J-P (1996) Cartes paléogéographiques-palinspastiques du bassin molassique suisse (Oligocène inférieur – Miocène moyen). *N Jahrb Geol Paläontol Abh* 202:1–44
- Berggren WA, Kent DV, Swisher CC, Aubry M-P (1995) A revised Cenozoic geochronology and chronostratigraphy. In: Berggren WA, Kent DV, Aubry M-P, Hardenbol J (eds) *Geochronology, time scales and global stratigraphic correlations*. *Soc Econ Paleontol Mineral Spec Publ* 54:17–28
- Berli S (1985) Die Geologie des Sommersberges (Kantone St. Gallen und Appenzell). *Ber St Gall Natf Ges* 82:112–145
- Blanckenburg F von (1992) Combined high-precision chronometry and geochemical tracing using accessory minerals: applied to the Central-Alpine Bergell intrusion (central Europe). *Chem Geol* 100:19–40
- Bolliger T (1992) Kleinsäugerstratigraphie in der lithologischen Abfolge der miozänen Hörnlischüttung (Ostschweiz) von MN3 bis MN7. *Eclogae Geol Helv* 85:961–1000
- Bolliger T (1994) Die Obere Süsswassermolasse in Bayern und in der Ostschweiz: bio- und lithostratigraphische Korrelationen. *Mitt Bayer Staatsslg Paläontol Hist Geol* 34:109–144
- Bolliger T, Kindlimann R, Wegmüller U (1995) Die marinen Sedimente (jüngere OMM, St.Galler-Formation) am Südwestrand der Hörnlischüttung (Ostschweiz) und die paläökologische Interpretation ihres Fossilinhaltes. *Eclogae Geol Helv* 88:885–909
- Büchi UP (1950) Zur Geologie und Paläogeographie der südlichen mittelländischen Molasse zwischen Toggenburg und Rheintal. PhD thesis, Universität Zürich, 99 pp
- Büchi UP (1956) Zur Geologie der Oberen Meeresmolasse von St. Gallen. *Eclogae Geol Helv* 48:257–321
- Büchi UP, Hofmann F (1960) Die Sedimentationsverhältnisse zur Zeit der Muschelsandsteine und Grobkalke im Gebiet des Beckennordrandes der Oberen Meeresmolasse zwischen Aarau und Schaffhausen. *Bull Ver schweiz Petrol Geol Ing* 27:11–22
- Büchi UP, Welti G (1951) Zur Geologie der südlichen mittelländischen Molasse der Ostschweiz zwischen Goldingertobel und Toggenburg. *Eclogae Geol Helv* 44:183–206
- Büchi UP, Wiener G, Hofmann F (1965) Neue Erkenntnisse im Molassebecken auf Grund von Erdöltiefbohrungen in der Zentral- und Ostschweiz. *Eclogae Geol Helv* 58:87–108
- Burbank DW, Engesser B, Matter A, Weidmann M (1992) Magnetostratigraphic chronology, mammalian faunas, and stratigraphic evolution of the Lower Freshwater Molasse, Haute-Savoie, France. *Eclogae Geol Helv* 85:399–431
- Bürgisser HM (1980) Zur Mittel-Miozänen Sedimentation im nordalpinen Molassebecken: das "Appenzellergranit"-Leitniveau des Hörnli-Schuttfächers (OSM, Nordostschweiz). PhD thesis, ETH Zürich, 196 pp
- Bürgisser HM (1981) Fazies und Paläohydrologie der Oberen Süsswassermolasse im Hörnli-Fächer (Nordostschweiz). *Eclogae Geol Helv* 74:19–28
- Bürgisser HM (1984) A unique mass flow marker bed in a miocene streamflow molasse sequence, Switzerland. In: Koster EH, Steel RJ (eds) *Sedimentology of gravels and conglomerates*. *Can Soc Petrol Geol Mem* 10:147–163
- Burkhard M (1990) Aspects of the large-scale Miocene deformation in the most external part of the Swiss Alps (Subalpine Molasse to jura fold belt). *Eclogae Geol Helv* 83:559–583
- Butler RF (1992) *Paleomagnetism*. Blackwell, Boston, 319 pp
- Cande SC, Kent DV (1992) A new geomagnetic polarity timescale for the late Cretaceous and Cenozoic. *J Geophys Res* 97:13917–13951
- Cande SC, Kent DV (1995) Revised calibration of the geomagnetic polarity timescale for the Late Cretaceous and Cenozoic. *J Geophys Res* 100:6093–6095
- Diem B (1986) Die Untere Meeresmolasse zwischen der Saane (Westschweiz) und der Ammer (Oberbayern). *Eclogae Geol Helv* 79:493–559
- Dietrich V (1969) Die Oberhalbsteiner Talbildung im Tertiär: ein Vergleich zwischen den Ophiolithen und deren Detritus in der ostschweizerischen Molasse. *Eclogae Geol Helv* 62:637–641
- Engesser B (1990) Die Eomyidae (Rodentia, Mammalia) der Molasse der Schweiz und Savoyens. *Systematik und Biostratigraphie*. *Schweiz Paläontol Abh* 112:1–144
- Fisher RA (1953) Dispersion on a sphere. *Proc R Soc Lond A* 217:295–305
- Frei H-P (1979) Stratigraphische Untersuchungen in der subalpinen Molasse der Nordost-Schweiz zwischen Wägitaler Aa und Urnäsch. *Mitt Geol Inst ETH Univ Zürich (NF)* 233:1–207
- Füchtbauer H (1958) Die Schüttungen im Chatt und Aquitan der deutschen Apenninmolasse. *Eclogae Geol Helv* 51:928–941
- Füchtbauer H (1964) Sedimentpetrographische Untersuchungen in der älteren Molasse nördlich der Alpen. *Eclogae Geol Helv* 57:157–298
- Gasser U (1967) Erste Resultate über die Verteilung von Schwermineralen in verschiedenen Flyschkomplexen der Schweiz. *Geol Rundsch* 56:300–308
- Giger M, Hurford AJ (1989) Tertiary intrusives of the Central Alps: their Tertiary uplift, erosion, redeposition and burial in the south-alpine foreland. *Eclogae Geol Helv* 82:857–866
- Gubler T, Meier M, Oberli F (1992) Bentonites as time markers for sedimentation of the Upper Freshwater Molasse: geological observations corroborated by high-resolution single-Zircon U–Pb ages. 172. Jahrestagung SANW Abstracts, pp 12–13

- Habicht K (1945a) Geologische Untersuchungen im südlichen sanktgallisch-appenzellischen Molassegebiet. Beitr Geol Karte Schweiz NF 83:1–166
- Habicht K (1945b) Neuere Beobachtungen in der subalpinen Molasse zwischen Zugersee und dem st.gallischen Rheintal. *Eclogae Geol Helv* 38:121–149
- Habicht K (1987) Internationales stratigraphisches Lexikon. Band I: Europa, Fasz. 7: Schweiz, 7b: Schweizerisches Mittelland (Molasse). Schweiz Geol Komm, Basel
- Hofmann F (1957) Untersuchungen in der subalpinen und mittelländischen Molasse der Ostschweiz. *Eclogae Geol Helv* 50:289–322
- Hofmann F (1976) Überblick über die geologische Entwicklungsgeschichte der Region Schaffhausen seit dem Ende der Jurazeit. *Bull Ver Schweiz Petrol Geol Ing* 42:1–16
- Homewood P, Allen P (1981) Wave-, Tide-, and current-controlled sandbodies of Miocene Molasse, western Switzerland. *Am Assoc Petrol Geol Bull* 65:2534–2545
- Homewood P, Allen PA, Williams GD (1986) Dynamics of the Molasse Basin of western Switzerland. *Int Assoc Sediment Spec Publ* 8:199–217
- Hurford AJ (1986) Cooling and uplift patterns in the Lepontine Alps South Central Switzerland and an age of vertical movement on the Insubric fault line. *Contrib Mineral Petrol* 92:413–427
- Johnson NM, Stix J, Tauxe L, Cervený PF, Tahirkheli RAK (1985) Paleomagnetic chronology, fluvial processes, and tectonic implications of the Siwalik deposits near Chinji Village, Pakistan. *J Geol* 93:27–40
- Jordan TE (1981) Thrust loads and foreland basin evolution, Cretaceous, western United States. *Am Assoc Petrol Geol Bull* 65:2506–2520
- Kälin D (1997) The Mammal zonation of the Upper Marine Molasse of Switzerland reconsidered. In: Aguilar J-P, Legendre S, Michaux J (eds) *Actes du Congrès Biochrom'97. Mém Trav EPHE Inst Montpellier* 21:515–535
- Keller B (1989) Fazies und Stratigraphie der Oberen Meeresmolasse (Unteres Miozän) zwischen Napf und Bodensee. PhD thesis, Bern, 402 pp
- Keller B, Bläsi H-R, Platt NH, Mozley PS, Matter A (1990) Sedimentäre Architektur der distalen Unteren Süsswassermolasse und ihre Beziehung zur Diagenese und den petrophysikalischen Eigenschaften am Beispiel der Bohrungen Langenthal. *Geol Ber Landeshydrol Geol* 13:1–100
- Kempf O (1998) Magnetostratigraphy and facies evolution of the Lower Freshwater Molasse (USM) of eastern Switzerland. PhD thesis, Bern, 138 pp
- Kempf O, Bolliger T, Kälin D, Engesser B, Matter A (1997) New magnetostratigraphic calibration of Early to Middle Miocene mammal biozones of the North Alpine foreland basin. In: Aguilar J-P, Legendre S, Michaux J (eds) *Actes du Congrès Biochrom'97. Mém Trav EPHE Inst Montpellier* 21:547–561
- Kleiber K (1937) Geologische Untersuchungen im Gebiet der Hohen Rone. *Eclogae Geol Helv* 30:419–430
- Leupold W, Tanner H, Speck J (1942) Neue Geröllstudien in der Molasse. *Eclogae Geol Helv* 35:235–246
- Ludwig A, Saxer F, Eugster H, Fröhlicher H (1949) Geologischer Atlas der Schweiz 1:25,000, Bl. 222–225 St. Gallen-Appenzell (Nr. 23). Schweiz Geol Komm, Basel
- Matter A (1964) Sedimentologische Untersuchungen im östlichen Napfgebiet (Entlebuch – Tal der Grossen Fontanne, Kt. Luzern). *Eclogae Geol Helv* 57:315–429
- Matter A, Homewood P, Caron C, Rigassi D, Van Stuijvenberg J, Weidmann M, Winkler W (1980) Flysch und Molasse of Western and Central Switzerland. In: Trümpy R (ed) *Geology of Switzerland, a guidebook* (part B). Schweiz Geol Komm, Wepf, Basel, pp 261–293
- Menkveld-Gfeller U (1997) Die Bürgen-Formation und die Klinsenhorn-Formation: Formelle Definition zweier lithostratigraphischer Einheiten des Eozäns der helvetischen Decken. *Eclogae Geol Helv* 90:245–261
- Miall AD (1991) Hierarchies of architectural units in terrigenous clastic rocks, and their relationship to sedimentation rate. In: Miall AD, Tyler N (eds) *The three-dimensional facies architecture of terrigenous clastic sediments and its implications for hydrocarbon discovery and recovery. Soc Econ Paleontol Spec Publ* 3:6–12
- Michalski I, Soom M (1990) The Alpine thermo-tectonic evolution of the Aar and Gotthard massifs, Central Switzerland: fission track ages on zircon and apatite and K–Ar mica ages. *Schweiz Mineral Petrogr Mitt* 70:373–387
- Milnes AG, Pfiffner OA (1977) Structural development of the Infralhelvetic Complex, eastern Switzerland. *Eclogae Geol Helv* 70:83–95
- Milnes AG, Pfiffner OA (1980) Tectonic evolution of the Central Alps in the cross section St. Gallen-Como. *Eclogae Geol Helv* 73:619–633
- Müller M, Nieberding F, Wanninger A (1988) Tectonic style and pressure distribution at the northern margin of the Alps between Lake Constance and the River Inn. *Geol Rundsch* 77:787–796
- Ochsner A (1975) Erläuterungen: Geologischer Atlas der Schweiz 1:25,000, Bl. 1133 Linthebene (Nr. 53). Schweiz Geol Komm, Basel
- Pfiffner OA (1985) Displacements along thrust faults. *Eclogae Geol Helv* 78:313–333
- Pfiffner OA (1986) Evolution of the north Alpine foreland basin in the Central Alps. *Int Assoc Sediment Spec Publ* 8:219–228
- Pfiffner OA, Hitz L (1997) Geologic interpretation of the seismic profiles of the Eastern Traverse (lines E1–E3, E7–E9): eastern Swiss Alps. In: Pfiffner OA, Lehner P, Heitzmann P, Mueller S, Steck A (eds) *Deep structure of the Swiss Alps: results of NRP 20. Schweiz Geol Komm, Basel*, pp 73–100
- Pfiffner OA, Erard PF and Stäubli M (1997a) Two cross sections through the Swiss Molasse Basin. In: Pfiffner OA, Lehner P, Heitzmann P, Mueller S and Steck A (eds) *Deep structure of the Swiss Alps: results from NRP 20. Schweiz geol Komm, Basel*, pp 64–72
- Pfiffner OA, Sahli S, Stäubli M (1997b) Structure and evolution of the external basement massifs (Aar, Aiguilles Rouges/Mt. Blanc). In: Pfiffner OA, Lehner P, Heitzmann P, Mueller S, Steck A (eds) *Deep structure of the Swiss Alps: results from NRP 20. Schweiz Geol Komm, Basel*, pp 139–153
- Renz HH (1937a) Die subalpine Molasse zwischen Aare und Rhein. *Eclogae Geol Helv* 30:87–214
- Renz HH (1937b) Zur Geologie der östlichen st. gallisch – appenzellischen Molasse. *Jahrb St Gall Natw Ges* 69:1–128
- Saxer F (1938) Die Molasse am Alpenrand zwischen der Sitter und dem Rheintal. *Eclogae Geol Helv* 31:373–375
- Schaad W, Keller B, Matter A (1992) Die Obere Meeresmolasse (OMM) am Pfänder: Beispiel eines Gilbert-Deltakomplexes. *Eclogae Geol Helv* 85:145–168
- Schlanke S (1974) Geologie der subalpinen Molasse zwischen Biberbrugg SZ, Hütten ZH, und Aegerisee ZG, Schweiz. *Eclogae Geol Helv* 67:243–331
- Schlunegger F, Matter A, Mange MA (1993) Alluvial fan sedimentation and structure of the southern Molasse Basin margin, Lake Thun area, Switzerland. *Eclogae Geol Helv* 86:717–750
- Schlunegger F, Burbank DW, Matter A, Engesser B, Mödden C (1996) Magnetostratigraphic calibration of the Oligocene to Middle Miocene (30–15 Ma) mammal biozones and depositional sequences of the Swiss Molasse Basin. *Eclogae Geol Helv* 89:753–788
- Schlunegger F, Leu W, Matter A (1997a) Sedimentary sequences, seismofacies, subsidence analysis, and evolution of the Burdigalian Upper Marine Molasse Group (OMM) of central Switzerland. *Am Assoc Petrol Geol Bull* 81:1185–1207
- Schlunegger F, Matter A, Burbank DW, Klaper EM (1997b) Magnetostratigraphic constraints on relationships between evolution of the central Swiss Molasse basin and Alpine orogenic events. *Geol Soc Am Bull* 109:225–241

- Schlunegger F, Matter A, Burbank DW, Leu W, Mange M, Mátys J (1997c) Sedimentary sequences, seismofacies and evolution of depositional systems of the Oligo/Miocene Lower Freshwater Molasse Group, Switzerland. *Basin Res* 9:1–26
- Schmid SM (1975) The Glarus overthrust: field evidence and mechanical model. *Eclogae Geol Helv* 68:247–280
- Schmid SM, Zingg A, Handy M (1987) The kinematics and movement along the Insubric line and the emplacement of the Ivrea zone. *Tectonophysics* 135:47–66
- Schmid SM, Aebli HR, Heller F, Zingg A (1989) The role of the Periadriatic Line in the tectonic evolution of the Alps. *Geol Soc Lond Spec Publ* 45:153–171
- Schmid SM, Pfiffner OA, Froizheim N, Schönborn G, Kissling E (1996) Geophysical–geological transect and tectonic evolution of the Swiss–Italian Alps. *Tectonics* 15:1036–1064
- Schmid SM, Pfiffner OA, Schönborn G, Froizheim N, Kissling E (1997) Integrated cross section and tectonic evolution of the Alps along the Eastern Traverse. In: Pfiffner OA, Lehner P, Heitzmann P, Mueller S, Steck A (eds) *Deep structure of the Swiss Alps: results of NRP 20*. Schweiz Geol Komm, Basel, pp 289–304
- Schoepfer P (1989) *Sédimentologie et Stratigraphie de la Molasse Marine Supérieure entre le Gibriloux et l'Aar*. PhD thesis, Fribourg, 211 pp
- Schwerd K, Huber K, Müller M (1995) Tektonik und regionale Geologie der Gesteine in der Tiefbohrung Hindelang 1 (Allgäuer Alpen). *Geol Bavarica* 100:75–115
- Sinclair HD, Coakley BJ, Allen PA, Watts AB (1991) Simulation of foreland basin stratigraphy using a diffusion model of mountain belt uplift and erosion: an example from the central Alps, Switzerland. *Tectonics* 10:599–620
- Sinclair HP, Allen PA (1992) Vertical versus horizontal motions in the Alpine orogenic wedge: stratigraphic response in the foreland basin. *Basin Res* 4:215–232
- Stäubli M, Pfiffner OA (1991) Processing interpretation and modeling of seismic reflection data in the Molasse Basin of eastern Switzerland. *Eclogae Geol Helv* 84:151–175
- Tanner H (1944) Beitrag zur Geologie der Molasse zwischen Ricken und Hörnli. *Mitt Thurgau Natf Ges* 33:1–108
- Vollmayr T, Jäger G (1995) Interpretation seismischer Daten und Modelle zur Vorbereitung und Auswertung der Bohrung Hindelang 1 (Allgäuer Alpen). *Geol Bavarica* 100:153–165
- Vollmayr T, Wendt A (1987) Die Erdgasbohrung Entlebuch-1, ein Tiefenaufschluss am Alpennordrand. *Bull Schweiz Ver Petrol Geol Ing* 53:67–79
- Woletz G (1967) Schwermineralvergesellschaftungen aus ostalpinen Sedimentationsbecken der Kreidezeit. *Geol Rundsch* 56:308–320
- Zingg A, Hunziker JC (1990) The age of movement along the Insubric Line west of Locarno (northern Italy and southern Switzerland). *Eclogae Geol Helv* 83:629–644